2012

Quantifying Glacier-Derived Summer Runoff in Northwest Montana

Adam Michael Clark
The University of Montana

QUANTIFYING GLACIER-DERIVED SUMMER RUNOFF IN NORTHWEST

MONTANA

By

Adam Michael Clark

B.A. Psychology, The University of Montana, Missoula, MT, 2006

A Thesis

presented in partial fulfillment of the requirements
for the degree of

Master of Science
in Geosciences

The University of Montana
Missoula, MT

November 2012

Approved by:

Sandy Ross, Associate Dean of The Graduate School

Joel T. Harper, Chair
Department of Geosciences

Johnnie N. Moore
Department of Geosciences

David D. Shively
Department of Geography

Daniel B. Fagre
U.S. Geological Survey

Clark, Adam, M.S., Fall 2012   Geosciences

Quantifying Glacier-Derived Summer Runoff in Northwest Montana

Chair: Joel T. Harper

  Glacier National Park, located in northwest Montana contains the second largest
concentration of glaciers in the U.S. Rocky Mountains. However, total glacier-covered
area has shrunk by almost 30% over the past 50 years. This has important implications
for local glacier-fed streams, especially during the typically hot and dry summer month of
August. This study is the first attempt to quantify the volume of glacier meltwater
entering local streams. We simulate glacier-melt generation during the summers of 2009
and 2010 using a modified temperature-index model that includes solar radiation as input.
The model was calibrated with data from weather stations installed on five different
glaciers and in situ measurements of surface ablation. Simulated glacier-melt hereafter
"glacier runoff" from within gauged basins was then compared to measured stream
discharge for the month of August to assess the relative contribution of glacier runoff to
stream flows. We find the fraction of August stream discharge potentially derived from
glaciers is not linearly proportionate to glacier cover. In watersheds only 0.12%
glacierized, glacier runoff equals 5%-6% of the August total discharge; glacier runoff is
23%-28% of the discharge in a stream draining a basin 1.4% glacierized; and, in the
small alpine catchments where glacier cover exceeds 25% of the basin area, glacier
runoff likely accounts for almost all of the total runoff. Our work suggests that during dry
summer months, glacier runoff is a primary control on both water availability and water
temperature in small alpine basins with a catchment area on the order of tens of km^2 and
smaller and that are located within 20 km of the continental divide. However, the
significance of meltwater diminishes quickly when travelling downstream and that in
larger rivers situated 50 km or more from glaciers, glacier runoff is minimally important.

ACKNOWLEDGEMENTS

TABLE OF CONTENTS

LIST OF FIGURES AND TABLES

FIGURES:

TABLES:

1. Introduction

Mountain glaciers in North America are reservoirs of snow and ice which store winter precipitation and release meltwater during summer months. They play a key role in the hydrology of the basins they occupy by modulating the timing and volume of runoff (Meier and Tangborn, 1961). Water from snow and ice melt can replace or "compensate for" the lack of precipitation during a dry season or even during a dry (Rothlisberger and Lang, 1987). Hence glaciers can moderate the effects of seasonal and long-term droughts. Even a small percentage of glacierized area within a basin can have substantial effects on runoff. For example, glacier meltwater comprises as much as 40% of the annual discharge in the Rio Santa watershed in the Peruvian Andes (Mark et al., 2005), and in the Brahmaputra and Indus Rivers in Central Asia (Immerzeel et al., 2010). These basins are just 8%, 3%, and 2% covered by glaciers, respectively.

The landscape within and bordering Glacier National Park, located in northwest Montana contain the second largest concentration of alpine glaciers in the U.S. Rocky Mountains (Figure 1). There are a total of 39 named glaciers, comprising 17.2 km^2 of glacierized area (USGS, unpublished data). All but two of these exist within Glacier National Park which was designated a Biosphere Reserve in 1976 and a World Heritage Site in 1995 due to the fact it contains an exceptionally large (4082 km^2) and intact natural ecosystem. Glacier melt runoff acts to cool streamflows, since water issuing from a glacier-outlet stream should be at, or very close to 0 °C (Paterson, 1994). This cold water is considered to be an integral part of this natural ecosystem, especially during the late summer months (Pederson et al., 2010; Muhlfeld et al., 2011). Bull trout, (*Salvelinus confluentus*) a native species in this region, require colder water compared to other North

1

American salmonids (Selong et al., 2001). Due to the projected impacts of a warming climate, they have already been listed as "threatened" under the Endangered Species Act (U.S Fish and Wildlife Service, 2012) . People also use this glacier meltwater. Irrigation demands in central Montana consume up to 75% of the discharge from the Saint Mary River (U.S. Bureau of Reclamation, 2012) which drains a basin containing two thirds of the total glacier area east of the continental divide. The glaciers west of the continental divide sit within the headwaters of the Columbia River watershed, a basin containing 31 hydroelectric facilities.

The retreat of glaciers in Glacier National Park has come to epitomize the impacts of a warming climate on the North American landscape and the hydrologic cycle. Glacier recession over the past 100 years has been well documented (Dyson, 1948; Johnson, 1980; Carrara and McGimsey, 1981). Recession rates here have been higher than in other U.S. mountain ranges (Fountain, 2007). With continued climate warming, glaciers are expected to continue shrinking or even disappear. One empirical projection estimates a complete melt-out of five glaciers by 2030 (Hall and Fagre, 2003), while another process-based model of a single glacier suggests it will last until 2080 under the most likely climate warming scenario (Brown et al., 2010). Milner and others (2009) argue that reductions in glacier-derived runoff will alter the spatial, temporal, and thermal characteristics of stream discharge, which in turn, threatens native species that evolved in glacier-fed streams. One study suggests the extinction of 11-38% of aquatic invertebrate species pools due to the loss of glaciers in a catchment (Jacobsen et al., 2012). Less glacier runoff will mean less water available for hydroelectric power generation and increased competition for water used to irrigate crops (Moore et al., 2009). Research

specific to the Glacier Park ecosystem denotes similar themes, inferring habitat loss for native cold-water aquatic species with possible extinctions if the glaciers disappear (Pederson et al., 2010; Muhlfeld et al., 2011).

Despite the numerous studies noted above describing the possible consequences of diminishing glacier ice in Glacier National Park, no research has attempted to quantify the past or present-day glacier melt runoff from this region. Thus, the fraction of runoff derived from glacier melt is unclear, leaving uncertainty to the hydrologic and ecological role of this region's glaciers. Hence, we must first understand the present-day role of glacier-melt runoff before we can adequately predict the future impacts that could result due to glacier recession.

Here we investigate the glacier-derived component to August runoff in the greater Glacier Park region. We develop methods to manage challenging mountain terrain with little to no in situ hydrologic or glaciological measurements. Our work yields essential knowledge of how present-day glaciers impact the regional hydrograph, and we interpret our results within the context of hydrological and ecological significance.

2. Methods

2.1. Study Glaciers

This study only includes glaciers that lie inside Glacier National Park, Montana with the exception of Stanton and Grant Glaciers, which sit within 10 km the park's western boundary (Figure 1, Appendix). Most glaciers here are wider than they are long relative to the flow direction, and would be classified as cirque and niche glaciers (Key et al., 2002). They exist primarily above 2000 meters and are located near the continental

divide in east to northeast-facing cirques with steep headwalls where they likely accumulate much of their mass from avalanching and wind-transported snow (Graf, 1976; Kuhn, 1995; Allen, 1998). Of the 39 glaciers, the average size is 0.44 km^2, but only 11 glaciers exceed this area: their range is 0.02 km^2 to 1.89 km^2 with a median size of 0.28 km^2. During any given year there are an undetermined number of other un-named snow and ice masses persisting through August, but our study is restricted to the 39 named glaciers. Only Sperry Glacier (~0.87 km^2) has a surface mass balance monitoring program, run by the U.S. Geological Survey (USGS). Measurements began in 2005 where the winter, summer, and net annual balances are quantified (USGS unpublished data).

2.2. Modeling Scheme

Quantifying glacier runoff across the region from glaciological techniques e.g. (Kaser et al., 2003) is not possible as mass balance data are available for just one glacier in the study area. The lack of glacier-outlet stream flow gauges also precludes the use hydrologic methods e.g. (Pellicciotti et al., 2010), where glacier melt is calculated as the residual from a basin water balance. These problems are common to glacierized areas and many studies turn next to model simulations of glacier melt as a proxy for runoff (Hock, 2005; Comeau et al., 2009; Huss, 2011). Our strategy here is to simulate melt from the glaciers based on meteorological data. This yields the total volume of potential runoff, but does no accounting for water storage within glaciers or losses to groundwater beneath glaciers. Hence, our modeled glacier melt is a maximum possible runoff.

We simulate surface melt of the 39 glaciers delineated on a digital topographic

landscape. Elevation data are derived from a 30 m resolution digital elevation model (DEM) obtained from the USGS and re-sampled to 60 m grid spacing for computational efficiency. The margin of each glacier was determined by hand-digitizing polygons using aerial photographs taken during the late summer when seasonal snow cover was minimal or absent (USGS unpublished data). Thirty two glacier polygons were obtained from vertical aerial photos taken in 2005, while the remaining seven came from vertical aerial photos taken in 1998. Some outlines were field checked for accuracy. These polygons are the most up to date measurements of glacier extent in this region.

While energy balance methods perform well for modeling melt at the point scale (Hock, 2005; Dewalle and Rango, 2008), they require high time and space resolution measurements of multiple meteorological parameters, making them difficult to upscale to regional simulations. Weather stations in this region are sparse, averaging 1 station per 480 km^2. We therefore chose to simulate glacier melt using a modified temperature-index model (Figure 2) which is based on the well-established empirical relationships between air temperatures, insolation, and glacier melt (Hock, 2003). On large spatial and temporal scales, these simpler, empirically-derived models typically out-perform physically-based, energy balance models (Ohmura, 2001; Hock, 2003). Compared to traditional temperature-index and/or degree-day models, the modified model includes the addition of a separate solar radiation term such that,

$$M = \alpha T + \beta SR \qquad\qquad T > T_c \qquad\qquad\qquad (1)$$

$$M = 0 \qquad\qquad\qquad T \leq T_c$$

Here, M is melt (md^{-1}), α is an empirically derived temperature coefficient ($md^{-1}C^{-1}$),

T is mean daily air temperature (°C), T_c is the critical temperature for melt (*0* °C), *SR* is cumulative daily solar radiation (*W*), *β* is an empirically derived radiation coefficient ($m d^{-1} W^{-1}$). The solar radiation component improves model performance because incoming solar radiation is a major source of heat energy that should be treated independently of air temperature (Hock, 1999; Pellicciotti et al., 2005). Unlike air temperature, which is more closely related to elevation, incoming solar radiation is strongly influenced by local topography.

Mean daily air temperatures from local weather stations (Figure 1; Table 1) were distributed across the model domain using an inverse-distance weighting interpolation combined with a linear lapse rate adjustment scheme (Dodson and Marks, 1997; Gillan et al., 2010) (see Appendix). In 2010, we installed five, high-elevation (ranging from 2058-2525 m) weather stations on five different glaciers in order to observe temperature, solar radiation, and make direct measurement of surface ablation. One product of these data was a locally derived lapse rate of 0.0074 °C m^{-1} (section 2.4.). To create the temperature grid, observed average daily air temperatures at each weather station are first converted to their respective sea level equivalents using the lapse rate and the DEM. The inverse-distance weighting equation (see Appendix) then interpolates an average daily temperature for each grid cell across the model domain. Each grid cell value is then converted back to its elevation-influenced temperature using the cell's altitude from the DEM and the local lapse rate.

The radiation index for each grid cell was obtained by first calculating the potential, direct solar radiation received for each hour in every grid cell. These calculations account for northing and easting coordinates, time of year/day, slope angle

and aspect, as well as shading effects due to the surrounding topography. Hourly values were then summed for each day. The clear sky potential radiation was then scaled each day by a different factor to account for daily changes in cloud cover. The scaling factor was derived from measurements of insolation collected at 5 different weather stations each year (Table 1; Appendix). In 2010 these weather stations were located on glaciers (section 2.4; Table 1).

The coefficients α and β were optimized (section 2.5.) using measurements of temperature, insolation, and glacier surface melt collected at the five instrumented glaciers during 2010. Equation 1 computes a depth in meters of meltwater for each grid cell (Figure 2) so multiplying this depth by the cell area yields a meltwater volume. Summation of the grid cells within each glacier polygon produces a total daily meltwater volume for each glacier, and summation of every glacier polygon gives a total volume of glacier runoff for the entire study area.

2.3. Study Interval

We run the model for months July-September, but focus our results on the month of August. August is the month when glacier runoff is most distinct from seasonal snow runoff and when the glacier derived component is most critical to the hydrograph. The snowpack lingers well into July above 2000 m (Gillan et al., 2010), with peak snowmelt runoff in late June. August is the 2nd warmest and driest month of the year, next to July. Low elevation (~1000m) sites with long-term meteorological records, show average August temperatures range from 15-17 °C and average monthly precipitation is 4-5 cm (Finklin, 1986). In September, mean temperatures drop and precipitation increases, both

changing 30% from August values (Finklin, 1986). With accumulating snowfall typically returning to high elevations, glacier melt shows a marked decline in most years (USGS unpublished data).

We model two contrasting years, 2009 and 2010. Based on data collected at Sperry Glacier, these two years represent relatively high and low melt years (USGS unpublished data). Therefore, averaging the model results from these two end-member years will give a robust approximation of what melt conditions are like during an average year. A weather station located within 200 meters of Sperry Glacier shows the average daily air temperature in August 2009 was 9.1 °C, which is 0.4 °C warmer than the 2006-2010 average. During August 2010, the average daily temperature was only 7.2 °C. In fact, August 2010 was the second coldest August on record and it had almost 2.5 times the average number of hours (29) when temperatures were 0 °C or colder. The Sperry Glacier summer balance (total water volume lost divided by glacier area) was 3.90 m in 2009. This was 0.50 m greater than the 2005-2011 average of 3.40 m, and 0.95 m greater than the 2010 value of 2.95 m.

Temperature records from Flattop SNOTEL and Kalispell Airport (Figure 1 and Table 1) show 2009 was warmer than average and 2010 was cooler, similar to the Sperry Glacier site. The average August temperature for the entire period of record (1985-2010) at the Flattop SNOTEL was 11.3 °C with a standard deviation of 1.8 °C. During this same 26-year period, the August mean at the Kalispell Airport was 17.5 °C with a standard deviation of 1.4 °C. 2009 was the 12th warmest August at Flattop (11.9 °C) and the 11th warmest at Kalispell (18.0 °C). Conversely, 2010 was the 19th warmest (or 8th coolest) August at both sites, with values of 10.8 °C at Flattop and 16.7 °C at Kalispell.

These data show that neither 2009 nor 2010 experienced extreme temperatures during

August given the longer period of record. Both months sit well within 1 standard

deviation of the mean. However, 2009 was still a relatively warm month compared to the

average conditions and 2010 was relatively cool. Furthermore, calculating an average

temperature at each site using only 2009 and 2010 gives a value within 1% of the mean

value derived from the entire period of record. This provides additional support to our

methods of modeling two contrasting high/low melt years and taking the average to

represent a typical melt season.

2.4. Field Measurements

From June 27th to September 11th, 2010 measurements of air temperature,

insolation, and glacier surface melt were taken on five different glaciers: Blackfoot,

Grinnell, Pumpelly, Sexton, and Sperry (Figure 3). The weather stations on Blackfoot

and Pumpelly Glaciers were removed on September 11th, but measurements continued

until September 25th on Grinnell Glacier, and until September 26th on Sexton and Sperry

Glaciers. These five glaciers were chosen to examine the effects of elevation, aspect, and

topographic shading on the measured variables (Table 3). We built a tower consisting of

three support legs with horizontal cross bars on each glacier. The legs were drilled 7

meters into the glacier using a back-packable steam drill. Sensors and a data logger were

attached to the structure and power was supplied by a battery and recharging 5 Watt solar

panel (Figure 4). A 0.1 °C-resolution thermistor inside a radiation shield measured

temperature and a pyranometer measured incoming solar radiation. Surface melt was

obtained with a sonic distance ranger, which measured the distance from the sensor

mounted on the structure to the glacier's surface. The height loss measured by the sonic

ranger multiplied by the density of snow or ice provided a water-equivalent depth for the

mass lost at that point. Measurements were taken every 10 minutes and then stored in the

data logger as hourly averages.

Fifteen ablation stakes were also installed on the glaciers (Figure 3). We visited

each glacier on 3-5 week rotations to lower the meteorological station instruments on

their support poles, and to measure the height loss and the remaining winter's snow depth

at each stake. Measurements of the winter snowpack allowed us to partition the fraction

of the season's melt as snow versus ice at each stake. To measure snow density we dug

four snow pits, one each on Sexton, Pumpelly, and Grinnell Glaciers during mid-July,

2010, and an additional snow pit on Sexton Glacier in mid-July, 2011. Snow pit depths

ranged from 1.0 m to 1.2 m and density measurements were made at 0.10 m intervals to

obtain an average bulk snow density which was 550 kg m^{-3}.

2.5. Coefficient Calibration

Data from the on-ice weather stations were compiled into daily values of mean air

temperature, cumulative insolation, and cumulative melt. From these data, we derived the

coefficients α and β iteratively using equation 2 and choosing the values of α and β that

correspond to the lowest sum of square errors (see Appendix).

$$\Phi = \Sigma_i \{(melt)_i - [(\alpha\ temp)_i + (\beta\ solar)_i\,]\}^2 \qquad\qquad (2)$$

Here, Φ is the sum of the squared errors between the daily measured meters of water equivalent on the ith day, ($melt_i$) and the modeled melt, the quantity inside square brackets. $Temp_i$ is the measured mean daily air temperature on the ith day, and $solar_i$ is the measured insolation for the ith day. The ranges of α (0.001-0.007) and β (3.0×10^{-7} – 1.0×10^{-5}) used in equation 2 were obtained from exploratory linear regressions made with the data beforehand. The optimal values for the month of August were 0.0038 md^{-1}C^{-1} for α and 3.93×10^{-6} m d^{-1} W^{-1} for β.

2.6. Comparisons to Streamflows

The potential contribution of glaciers to the total basin runoff was assessed by comparing the computed glacier unoff from catchments where the total basin runoff was measured by USGS stream gauges. For each gauged basin, glacier runoff from the glaciers lying within the catchment was summed for an August total. This was then divided by the total basin runoff measured at the gauge. We do not attempt to estimate the large amount of glacier-derived runoff lost to groundwater, evapotranspiration, and lake storage, or the lag time for glacier runoff to flow through the gauge. Hence, our aim is to provide a point of reference for a simple assessment of the potential relevance of glacier-derived runoff.

The study area is divided into five gauged watersheds (Table 2 and Appendix): North Fork Flathead River (NF), Middle Fork Flathead River (MF), Saint Mary River (SM), Swiftcurrent Creek (SW), and Upper Grinnell Creek (GC). Two other watersheds: the Belly and Waterton River basins are 1.0% and 0.5% glacierized respectively, and this study does model runoff from glaciers within those basins. However, these basins lack

11

useful stream gauge data, so we are unable to determine the relative proportion of total runoff that could be derived from glaciers. The NF and MF are the two largest watersheds, existing west of the continental divide and also having the smallest percentages of glacier-covered area. East of the continental divide, the SM watershed is the third largest basin and streamflows travel northeast to the South Saskatchewan River and eventually out to Hudson Bay. The SW catchment is a sub-basin of the SM watershed. The GC catchment is a sub-basin within SW basin and thus nested within the SM catchment and has the smallest catchment area and the highest percentage of glacierized area (~29%). This basin has the only glacier outlet stream with discharge data within the study area, but there are no records for 2009 and 2010. We used an average August discharge value from the most recent period of record, years 2004-2007 to represent the total basin runoff.

3. Results

3.1. Field Data

The five weather stations installed on glaciers in 2010 provide unique in situ point measurements of meteorological conditions and surface melt on daily time steps. Removal of elevation effects on the average daily air temperature by normalizing data from the five on-glacier weather stations to their mean elevation (2287 m) using the locally calculated lapse rate, indicates that mean daily temperatures vary little between stations across the landscape (Figure 5a). However, variability among stations is greater on an hourly time scale (e.g., Figure 5b and 5c). Further, average temperatures vary widely over time, and can change by as much as 15 °C between days.

The daily melt rate from sonic rangers during the period June 27th – September 26th, 2010 averages 0.035 m of water equivalent (w.e.) per day between all five sites, with a standard deviation of 0.016 m d^{-1} w.e. (Table 3). Plotting the cumulative daily melt from the five stations during this time period (Figure 6) shows the variability of glacier melt in space and time. From late June to late July, the average melt rate between the 5 stations was 0.043 m d^{-1} w.e., dropping to 0.037 m d^{-1} w.e. during late July to late August. Mean daily melt drops dramatically to 0.017 m d^{-1} w.e. from late August to late September if only melting days are included. If all days are included in the mean value, then the glaciers actually accumulated water at these points by an average rate of 0.003 m d^{-1}.

Ablation rates measured at the 15 stakes generally agree with results from the sonic ranger (Table 4), although comparisons are limited by the coarse time resolution of the stake measurements. Stake averages from late June to mid-July show the melt rate was 0.036 m d^{-1} w.e., rising to 0.044 m d^{-1} w.e. during mid-July to mid-August, then dropping to 0.017 m d^{-1} w.e. from mid-August to late September. The seasonal average (6/27 – 9/26) using the combined data was 0.033 m d^{-1} w.e.

3.2. Error Assessment

Since there are no discharge measurements available for 2009 and 2010 at the Upper Grinnell Creek gauge, we cannot compare our modeled glacier runoff to direct in-situ measurements of glacier runoff. Furthermore, meltwater from most other glaciers typically issues from many small outlets and often over cliffy terrain, thereby making discharge measurements unfeasible at other locations. Therefore, we rely upon

comparisons of model output to in-situ glacier surface melt measurements and tests for sensitivity of our results to uncertainties.

To investigate the sensitivity of our results to our optimized coefficients α and β, we ran the model using a range of coefficients (Table 5). Values for α and β were adjusted at 2% increments from +10% to -10%, and the model was run 20 times with random pairings of values (Figure 7). The greatest change occurred when α and β were simultaneously increased by 10%, which led to a 10% increase in all daily values of melt and total modeled runoff for the month of August. The model is more sensitive to changes in α than to changes in β. For example, a 10% increase in α and a 10% decrease in β gives an overall 3% increase in August runoff.

To examine the sensitivity of our results to interpolations of temperature and solar radiation we compare modeled to measured data. We omitted data from the five on-ice meteorological stations from the calculation of gridded data. This was done to assess our method's ability to simulate values at high-elevation sites (on glaciers) using only observations from low-to-mid elevation sites that are mostly located near the outskirts of the park and thus several tens of kilometers from the glaciers. The new gridded values were then compared to corresponding measurements at the on-ice stations. The residuals were normally distributed and for 53% of days, the measured temperatures were warmer than the interpolated values. The average difference was 2.0° C with a standard deviation of 1.4° C. The remaining 47% of the time, temperatures at the on-ice stations were colder by an average 1.7° C and a standard deviation of 1.7° C. When the solar radiation index was compared to the glacier weather stations, the average difference was 500 watts with a standard deviation of 400 watts. Again, the periods of more/less solar radiation

were split almost equally in half, with 51% of the days receiving more radiation than modeled and 49% of the days receiving less.

The uncertainties in both temperature and radiation can be combined to produce a total uncertainty in the results introduced by model input. If on average, the temperature and solar radiation indices differed from actual conditions by 2° C and 500 watts, this would translate to a difference of ± 0.01 m d^{-1} in meltwater equivalent on each grid cell. If this difference is assumed uniform across the study area, the total glacier runoff would change by 24% of the 2010 total and 19% of the 2009 total, both of which are substantial. However, these estimates assume that both the temperature and radiation indices are concurrently either too high or too low every day, which has a low probability of occurring. Our data show that over the entire month, the periods of positive and negative variations between model input and observations of temperature and solar radiation are almost equal, creating a "cancellation effect" where melt is over-computed half the time and under-computed the other half. Hence these estimates of uncertainty are likely very much upper limits.

We also compare our in-situ measurements of glacier melt at each ablation stake to the modeled melt from every grid cell containing a stake. Modeled results, in our case produced at a 60 m resolution, represent an average value for a 3600 m^2 area, while the stake readings represent only a specific point value within that area. Stake measurements also represent mass lost to sublimation and height loss due to snow densification; while our model results assume all height loss is due to melt. However, assuming a point measurement represents the average melt rate of the grid cell e.g. (Hock, 1999), supplies beneficial information about model error. In 2010, the model calculates melt to within

5% of the measured values at 8 of the 15 grid cells during the 7/10 – 8/16 time period. In 6 of these cells, modeled melt was within 1-3% of the measured, and at one cell there was no difference between the two. All stakes considered, percent differences ranged from -37 to 5%, but in only two cells was the difference more than -12%. Here a negative value indicates the model over-computed melt, which it did in ten of the fifteen cells. Thus, the mean percent difference was -7%, but the median was -3%. In 2009 we have seven stakes located on Sperry Glacier for comparisons. Percent differences ranged from -22% to 28% for the time period 7/22 – 8/24. The model over-simulated melt in three cells for an average value of 14% and under-computed melt by an average of 12% in the four other cells. The average percent difference using all stakes shows a much lower overall error of 1%.

Comparing modeled melt to the USGS summer balance on Sperry Glacier, suggests model performance improves significantly when considered at larger spatial and temporal scales. The USGS calculates the summer balance by interpolating surface melt at a 10 m^2 resolution using a kriging algorithm and point measurements of melt at 7 ablation stakes. Comparisons between the modeled summer balance (output from July, August, and September) from this study against the USGS balance are encouraging. The modeled summer balance for 2009 was 4.00 m while the USGS balance was 3.90 m, a difference of 3%. In 2010, the modeled summer balance was 2.80 m and the USGS balance was 2.95 m, a 5% difference.

Results from our error assessment demonstrate the strengths and limitations of our modeling approach. The largest potential for error is introduced by the temperature and solar radiation indices (±19-24%), with the model coefficients adding additional potential

error (±10%). Thus, daily melt at a single grid cell likely has a high amount of associated

error, perhaps as much as ±34%. However, as typical of temperature index models,

model performance improves at larger spatial scales (km^2) and longer time steps (weeks),

with errors down to ±7% and even as low as ±3% due to the cancellation effects

described above. For these reasons we argue this model is sufficient for our intended

purposes: to quantify the glacier-derived component to monthly streamflows from 17.2

km^2 of glacierized area.

3.3. Glacier Runoff

We calculate the total volume of glacier-derived runoff from all 39 glaciers (see

Appendix for list of runoff from each glacier) for August 2009 to be 28.37 $x10^6$ m^3 and

the 2010 August volume to be 21.92 $x10^6$ m^3. The average meltwater volume produced

each day (monthly total divided by 31 days) was 9.2 $x10^5$ m^3 in 2009 and 7.1 $x10^5$ m^3 in

2010, a difference of 23%. There were 14 days during August, 2009 when the total

region-wide glacier runoff exceeded 1.0 $x10^6$ m^3, with all but four of these days occurring

during the second half of the month. The day with the highest runoff was August 22nd

with a value of 1.31 $x10^6$ m^3. During the cooler month of August 2010, the highest melt

day landed on the 26th with a total volume of 1.17 $x10^6$ m^3. The lowest runoff days

occurred on the 15th in 2009 (3.5 $x10^5$ m^3) and on the 31st in 2010 (7 $x10^4$ m^3).

Records from nine regional weather stations (see Appendix), show peak melt days

were associated with exceptionally high temperatures with little (<3 mm) or no

precipitation. Mean daily air temperatures on these dates ranged from 1-6 °C above the

normal monthly averages. Conversely, the lowest melt days corresponded with cool and

often wet weather. Here, mean daily air temperatures were 1-9 °C lower than the monthly average with 6 stations in 2009 and 7 in 2010 reporting 2-13 mm of precipitation.

The average August specific discharge (glacier runoff volume divided by glacier area) considering all 39 glaciers was 1.68 m in 2009 and 1.33 m in 2010. August 2010 was slightly less variable with a standard deviation of 0.17 m versus 0.19 m in 2009. The maximum values on individual glaciers were 2.15 m during 2009 and 1.85 m during 2010. Both of these occurred on Lupfer Glacier, the lowest elevation glacier in the study area (mean altitude 1940 m). Minimum values were 1.26 m during 2009 and 1.00 m during 2010, both on the Hudson Glacier, interestingly the 11th lowest elevation glacier with a mean altitude of 2223 m. A correlation between mean monthly specific discharge and mean altitudes does exist, but it is not particularly strong (see Appendix). In general, a 1 meter climb in altitude results in a 0.002 m decline in monthly specific discharge. Daily specific discharges (monthly specific discharge divided by 31 days) averaged 0.053 m for 2009 (standard deviation 0.006 m) and 0.043 m for 2010 (standard deviation 0.006 m).

We did not find a relationship between specific discharge and glacier aspect. A contributing factor may be that there are no glaciers facing primarily due south. After controlling for elevation, glaciers with more southern exposures did not consistently produce more water than glaciers with more northerly ones. For example, the Harrison Glacier (mean elevation 2494 m) faces primarily southeast and the mean monthly specific discharge is 11% greater than the Kintla Glacier (mean 2540 m) but 2% lower than Sperry Glacier (mean 2460 m), both of which face predominantly north. A more dominant factor to summertime melt may be topographic shading. As noted above, the

Hudson Glacier is one of the lowest elevation glaciers among the 39 but it had the lowest specific discharge for both 2009 and 2010. This glacier sits in an almost due north facing cirque with steep headwalls rising 200-300 meters above it. This would reduce the solar radiation received at the ground surface and likely had an effect on melt rates.

3.4. Relative Contribution of Glacier Runoff Between Basins

The North Fork (NF) of the Flathead River basin is 3960 km^2. This is the largest basin in the study area and has the lowest amount of glacierized area at only 0.12% (Table 2). A stream gauge sits on a low-elevation (959 m) reach approximately 6 km from the basin outlet which is near Columbia Falls, Montana. Here, the nearest glacier is about 55 km away via the stream course (river km). Assuming all meltwater generated by glaciers within the basin flowed by the gauge, glacier-derived runoff would account for 6.3% of total discharge in 2009 and 5.0% of the total discharge in 2010 (Figure 8 and Table 6). In the next largest catchment, the Middle Fork of the Flathead (MF) at 2922 km^2 and at 0.16% glacierized with the nearest glacier 33 river km away, glacier runoff could account for 7.5% of total August flows in 2009 and 6.3% in 2010.

East of the continental divide, in the Saint Mary River (SM) watershed, the closest glacier is 31 river km from the stream gauge. This is the third largest basin at 715 km^2 and it is 0.70% glacierized. Here, as much as 13% of August discharge could originate as glacier melt during a hot and dry summer like that of 2009, whereas in 2010, it could only be as much as 9%. In the Swiftcurrent Creek (SW) watershed (80 km^2), currently 1.4% of the catchment is covered by ice and the closest glacier is 9 km away from the gauge. Here the potential relative contribution of glacier runoff rises

considerably, ranging from 28% in 2009 to 23% in 2010. In the smallest catchment, at the

Upper Grinnell Creek (GC) gauge, the modeled glacier runoff during August 2009

exceeded the total basin runoff, with a relative contribution of 109%. The gauge sits

within 500 m of Grinnell Glacier, but a 0.33 km^2 pro-glacial lake sits between it and the

ice. The greater than 100% value indicates that melt might be lost to other sinks such as

storage within the lake and the glacier. It is likely also evidence for error in the model

output and the fact we used an average from 2004-07 to represent basin runoff in the

absence of 2009 stream gauge data. In the cooler month of August 2010, the glacier

runoff component was still quite high at just over 85%.

When the percent of the catchment area glacierized is plotted against the percent

of the total runoff from each respective basin that is glacier-derived we found a non-

linear relationship (Figure 9). However, when these values are plotted on log base 10

axes, the relationship is very near linear and can be approximated well by the function R_g

$= 0.527A+1.23$ (Figure 10), where R_g is the logarithm of the percentage of total basin

runoff that could potentially come from glaciers and A is the logarithm of the percentage

of the basin glacierized. This relationship was found statistically significant using a t-test

with 95% confidence intervals, resulting in p-values < 0.0001.

4. Discussion

4.1. Present Glacier Contributions

Our findings indicate that even very small glaciers can have disproportionately

large effects on basin runoff, which agrees with similar other studies. For example, Nolin

and others (2010) concluded that glacier-derived runoff made up 41%-73% of the

discharge in the Upper Middle Fork of the Hood River which drains a basin only 6.6% glacierized in northern Oregon. Huss (2011) calculated glacier-melt contributions to rivers draining the European Alps and found that even in basins that were minimally glacierized e.g. 0.20% and 0.06%; glacier runoff still supplied 6.6% and 2.8% of the total August discharge, respectively. In the Canadian Rockies closer to our study area, glacier-melt can account for as much as 27% of the total runoff in basins as little as 1% glacierized (Comeau et al., 2009). This figure is comparable to the Swiftcurrent Creek basin in our study area.

The results from this study provide a quantitative understanding of the significance that glacier-runoff has on the hydrologic cycle in northwest Montana. This knowledge allows us to examine the roles that glacier runoff may have with respect to aquatic ecosystems and human uses of water that is sourced in Glacier Park.

The impact on streamflow volumes and temperatures is likely significant in the small, high-elevation streams located within 10 km of glaciers. For example, in the upper North Fork River watershed, bull trout spawn and rear in small streams beginning in August (Downs, 2011). D'Angelo (2010) searched for spawning bull trout in 79 different stream reaches within the North Fork River basin inside Glacier Park. Bull trout were found in only ten reaches, and four of these were in relatively high-elevation streams (>1200 m) located within 6 km of a glacier's terminus. These streams drained basins that are currently 3-6% glacierized. Our results from the nearby Swiftcurrent Creek watershed (1.4% glacierized) shows glacier melt potentially makes up 26% of August stream discharge, suggesting the glacier runoff component in the bull trout streams noted in the D'Angelo (2010) study is surely higher. These findings indicate glaciers are likely

valuable to bull trout because they are providing cold meltwater runoff to the high elevation spawning streams during a typically hot and dry time of year.

However as one moves downstream and further away from the glaciers, the impacts of glacier runoff on the larger, low elevation streams becomes much less. Again, at the stream gauge on the North Fork River proper, the nearest glacier is more than 55 river km away. Here the effect of glacier runoff on water temperatures can be examined by setting up a calorimetry problem (see Appendix). The following example is based on a partially theoretical scenario which assumes 100% of the glacier runoff reaches the stream gauge, but it illustrates the maximum possible effect. Using the mean August water temperature of 15.0 °C (std dev of 1.5 °C) measured at the gauge and assuming 100% of the glacier meltwater made it to this point still at 0 °C, our results show that the relatively small proportion of glacier runoff here would only act to cool the water by 0.8 °C, or about 5%. Observations on different tributary streams located within the North Fork River basin show average August water temperatures in glacier outlet streams can warm to 7-8 °C in as little as 4-6 km from the terminus (D'Angelo, 2010). Furthermore, measurements from this same study, taken in four glacier-fed streams near their confluences with the North Fork River, showed water temperatures had already reached 16-17 °C. Thus we conclude that glacier runoff has little influence on water temperature in the main body of the North Fork River.

Use of glacier runoff is not limited to aquatic species inside Glacier National Park. About 9 km east of the park's eastern boundary a canal diverts up to 75% of the Saint Mary River discharge into the North Fork of the Milk River during the months April through October. This water is used to irrigate approximately 570 km^2 of cropland

in central Montana. Our study shows that potentially 9%-13% of August discharge near the canal intake originates as glacier-melt. This is a non-trivial volume when considering the current demands of this water.

4.2. Historic Glacier Contributions

We also simulated glacier-derived runoff during the 1960's when the glaciers were larger and compared results to the present-day conditions. As the number of weather stations present within the park 50 years ago was insufficient to employ our modified temperature-index model, we must employ a simple melt rate/area scaling argument to estimate change in glacier runoff. Glacier extent in the 1960's was obtained by hand-digitizing glacier polygons using USGS maps that were drawn from aerial photographs taken in 1966 (USGS unpublished data). Next we used the averaged 2009-2010 August meltwater volumes from each individual glacier as a reference value representative of present-day runoff. Each glacier's respective change in area since 1966 was then used to scale up this reference runoff to account for the glacier's change in size from present day. For example, if a glacier was 35% larger in 1966, then the August meltwater volume was increased by 35%. USGS streamflow records provided the total basin runoff and this was used to calculate a ten year average for the years 1960-1969. For each gauged basin, the glacier runoff from the glaciers lying within the catchment was again summed for an August total and then divided by the total basin runoff.

In the two largest basins, the percent glacierized area in the 1960's was 0.17% in the North Fork, and 0.20% in the Middle Fork, as opposed to 0.12% and 0.16% respectively today. Glacier-derived runoff was 27% higher in the 1960's in the North

Fork catchment and 19% higher in the Middle Fork. In the North Fork, this equates to an increase in the percentage of total river discharge that could be glacier-derived from 5.6% for the present-day to 6.8% in the 1960's (Figure 8 and Table 6). In the Middle Fork basin the potential glacier runoff contributions changed from 6.9% to 7.9% in the 1960's. In the Saint Mary watershed, glacier runoff was 30% higher during the 1960's while glaciers covered 1.0% of the basin as opposed to 0.7% of the basin now. This would mean glacier runoff could potentially account for 12.7% of the total basin runoff 50 years ago instead of 10.7% as found for today's conditions. In the Swiftcurrent Creek catchment, the discrepancy between present-day and the 1960's is even greater. Here glaciers covered 2.1% of the catchment area during the 1960's and results show glacier runoff was also about 32% higher. Dividing the glacier runoff by total basin runoff shows that potential glacier contributions were over 30% during this decade as opposed to about 25% for the present-day.

In the Upper Grinnell Creek catchment, glaciers covered 44.7% of the catchment area during the 1960's and glacier-runoff was almost 36% higher. However, when glacier runoff is compared to the stream gauge record, we found that glacier-melt only made up about 85% of the total basin runoff in the 1960's as opposed 98% for the present-day. We attribute this finding to the errors associated with our crude methods used to calculate glacier runoff for the 1960's. It is reasonable to assume, given our model results for 2009 & 2010 and the fact that there are no other sources of water to this basin other than precipitation, that during the typically dry month of August, most all of the runoff in this stream is derived from glacier melt. A comparison between the two periods of record at the stream gauge (1960-1969 and 2004-2007) show mean August

runoff has decreased by about 46%. We argue that the changes observed in stream discharge provide a more accurate assessment of how glacier runoff has dropped over the past 50 years. We note the short dataset for the most recent measurement period and acknowledge that this may have influenced our findings. However, this is the only data available, and we conclude that our modeling results for 1960's glacier runoff are likely too low. This also suggests that the 50-year changes given above for the other basins are probably low-end estimates as well.

Our findings show that despite the fact glaciers here have receded on average by 35% since the 1960's (see Appendix), with some glaciers shrinking as much as 77%, the volumetric changes to glacier-derived runoff has likely had a very small impact on the larger rivers (e.g. North and Middle Forks of the Flathead) situated far from the ice and draining basins on the order of 10^2 and 10^3 km^2. However, in smaller glacier-fed streams, such as Swiftcurrent and Upper Grinnell Creeks, which drain basins on the order of tens of km^2 and smaller, the loss of glacier area and associated glacier-melt runoff has had a much more pronounced effect on the hydrograph.

4.3. Future Glacier Contributions

In the North Fork and Middle Fork watersheds, the two largest basins in the study area, the coefficient of variation of annual August discharge is about 5 times greater than the fraction of runoff that could potentially be glacier-derived (Table 2). Considering this inter-annual variability which encompasses all sources and sinks of water, it appears that a loss of glacier runoff would not have a major effect on August flows. For example, if glaciers were to disappear from the North Fork and Middle Fork watersheds, these rivers

25

are not likely to become un-navigable in the late summer. Nor will the loss of glacier-runoff have any lasting impact on water temperatures in these rivers.

On the other hand, if glaciers are gone from the smaller, high-elevation watersheds, then glacier-outlet streams like Upper Grinnell Creek would dry up as the winter's snowpack melts. This would cause habitat loss and fragmentation for aquatic insects such as caddisflies (Lowe and Hauer, 1999) and the meltwater stonefly, which is unique to Glacier Park and lives almost entirely in stream reaches that are within 500 meters of melting snow and ice (Muhlfeld et al., 2011). A continued loss of glacier meltwater will cause late summer flows to drop and water temperatures to rise in streams historically suitable for bull trout spawning. Bull trout are already threatened by the loss of thermally suitable habitat (Rieman et al., 2007). A complete melt-out of this region's glaciers will likely only further stress bull trout considering the work done by D'Angelo (2010) where fish were only found in only 10 of the 79 surveyed stream reaches with 4 of these reaches located in glacier outlet streams draining small basins that were greater than 3% glacierized.

Furthermore, the loss of glacier runoff could also exacerbate a predicted water shortage for farmers in central Montana who use the Saint Mary River to irrigate crops. A 2012 study done by the U.S. Department of the Interior-Bureau of Reclamation expected agricultural demands of Saint Mary River water to increase by 24%-29% by the year 2050. If glaciers were to vanish, August discharge in the Saint Mary could drop by as much 13%, creating an even smaller source of water from which to draw upon.

5. Conclusions

Due to a climate characterized by high temperatures and low precipitation during late summer, the small glaciers in and around Glacier National Park add a relatively large volume of water to August stream flows. Depending on ice coverage, the maximum possible contributions to August streamflows during an average year range from 6% in basins as little as 0.12% glacierized (North Fork of the Flathead) to 26% in basins that are still only 1.4% glacierized (Swiftcurrent Creek). In high-elevation, alpine watersheds, where glacier cover nears 30% of the basin area, glacier-melt is likely responsible for the majority of August runoff.

A conservative, low-end estimate suggests that glacier recession over the past 50 years has only reduced the glacier-derived component to August streamflows by 1-2% in large ($10^2 – 10^3$ km^2) basins that were 1% glacierized or less. In smaller catchments on the order of tens of km^2, the reduction in glacier area has decreased the glacier-derived component by about 5%. However, the loss of ice covered area may have reduced average August flows by more than 40% in a reach on a glacier-fed stream situated a few hundred meters from the terminus.

Our work reveals that a complete melt out of the region's glaciers would likely have negative impacts on species such as bull trout due to the resultant loss of cold meltwater discharge in spawning streams located within 10 km of glaciers. Diminishing glacier-melt runoff could also create increasing competition for Saint Mary River water used for agriculture. However, in large streams such as the North and Middle Forks of the Flathead River, a complete disappearance of glaciers would only minimally impact

discharge. Further, the effect on water temperatures in these two rivers would be negligible.

6. References Cited

Allen, T. R., 1998: Topographic context of glaciers and perennial snowfields, Glacier National Park, Montana. *Geomorphology,* 21(3): 207-216.

Brown, J., Harper, J., and Humphrey, N., 2010: Cirque glacier sensitivity to 21st century warming: Sperry Glacier, Rocky Mountains, USA. *Global and Planetary Change,* 74(2): 91-98.

Carrara, P. E. and McGimsey, R. G., 1981: The late-neoglacial histories of the Agassiz and Jackson Glaciers, Glacier National Park, Montana. *Arctic and Alpine Research* 183-196.

Comeau, L. E. L., Pietroniro, A., and Demuth, M. N., 2009: Glacier contribution to the north and south Saskatchewan rivers. *Hydrological Processes,* 23(18): 2640-2653.

D'Angelo, V. S., 2010: Factors influencing the distribution of bull trout and westslope cutthroat trout west of the continental divide in Glacier National Park. Master's Thesis, Environmental Studies, The University of Montana, Missoula, Montana. 60 pp.

Dewalle, D. R. and Rango, A., 2008: Principles of snow hydrology. Cambridge, UK: Cambridge University Press. 410 pp.

Dodson, R. and Marks, D., 1997: Daily air temperature interpolated at high spatial resolution over a large mountainous region. *Climate Research,* 81-20.

Downs, C., 2011. Glacier Natl. Park Fisheries Biologist. personal communication.

Dyson, J. L., 1948: Shrinkage of Sperry and Grinnell Glaciers, Glacier National Park, Montana. *Geographical Review,* 38(1): 95-103.

Finklin, A. I., 1986: A Climatic Handbook for Glacier National Park: With Data for Waterton Lakes National Park. U.S.D.o. Agriculture (ed.). Ogden, UT: Forest Service Intermountain Research Station, 124.

Fountain, A. G., 2007: A century of glacier change in the American West. *EOS Trans. of the American Geophysical Union,* 88(52).

Gillan, B. J., Harper, J. T., and Moore, J. N., 2010: Timing of present and future snowmelt from high elevations in northwest Montana. *Water Resources Research,* 46(1): WO1507.

Graf, W. L., 1976: Cirques as glacier locations. *Arctic and Alpine Research,* 8(1): 79-90.

Hall, M. H. P. and Fagre, D. B., 2003: Modeled climate-induced glacier change in Glacier National Park, 1850-2100. *BioScience,* 53(2): 131-140.

Hock, R., 1999: A distributed temperature-index ice and snowmelt model including potential direct solar radiation. *Journal of Glaciology,* 45(149): 101-111.

Hock, R., 2003: Temperature index melt modelling in mountain areas. *Journal of Hydrology,* 282(1): 104-115.

Hock, R., 2005: Glacier melt: a review of processes and their modelling. *Progress in physical geography,* 29(3): 362.

Huss, M., 2011: Present and future contribution of glacier storage change to runoff from macroscale drainage basins in Europe. *Water Resources Research,* 47(7): WO7511.

Immerzeel, W. W., Van Beek, L. P. H., and Bierkens, M. F. P., 2010: Climate change will affect the Asian water towers. *Science,* 328(5984): 1382-1385.

Jacobsen, D., Milner, A. M., Brown, L. E., and Dangles, O., 2012: Biodiversity under threat in glacier-fed river systems. *Nature Climate Change,* 2(5): 361-364.

Johnson, A., 1980: Grinnell and Sperry Glaciers, Glacier National Park, Montana: a record of vanishing ice. U.S.D.o. Interior. Geological Survey (ed.). Washington DC: United States Government Printing Office, 29.

Kaser, G., Fountain, A., Jansson, P., Heucke, E., and Knaus, M., 2003: A manual for monitoring the mass balance of mountain glaciers: Unesco.

Key, C. H., Fagre, D. B., and Menicke, R. K., 2002: Satellite image atlas of glaciers of the world, glaciers of North America - Glaciers of the western United States. U.S.D.o.Interior. Geological Survey (ed.). Washington DC: U.S. Government Printing Office, J365-J381.

Kuhn, M., 1995: The mass balance of very small glaciers. *Zeitschrift fur Gletscherkunde und Glazialgeologie,* 31(1): 171-179.

Lowe, W. H. and Hauer, F. R., 1999: Ecology of two large, net-spinning caddisfly species in a mountain stream: distribution, abundance, and metabolic response to a thermal gradient. *Canadian Journal of Zoology,* 771637-1644.

Mark, B. G., McKenzie, J. M., and Gomez, J., 2005: Hydrochemical evaluation of changing glacier meltwater contribution to stream discharge: Callejon de Huaylas, Peru. *Hydrological Sciences Journal,* 50(6): 975-987.

Meier, M. F. and Tangborn, W. L., 1961: Distinctive characteristics of glacier runoff. U.S.D.o. Interior. Geological Survey (ed.), 14-16.

Milner, A. M., Brown, L. E., and Hannah, D. M., 2009: Hydroecological response of river systems to shrinking glaciers. *Hydrological Processes,* 23(1): 62-77.

Moore, R. D., Fleming, S. W., Menounos, B., Wheate, R., Fountain, A., Stahl, K., Holm, K., and Jakob, M., 2009: Glacier change in western North America: influences on hydrology, geomorphic hazards, and water quality. *Hydrological Processes,* 23(1): 42-61.

Muhlfeld, C. C., Giersch, J. J., Hauer, F. R., Pederson, G. T., Luikart, G., Peterson, D. P., Downs, C. C., and Fagre, D. B., 2011: Climate change links fate of glaciers and an endemic alpine invertebrate. *Climatic Change,* 106337-345.

Nolin, A. W., Phillippe, J., Jefferson, A., and Lewis, S. L., 2010: Present-day and future contributions of glacier runoff to summertime flows in a Pacific Northwest watershed: Implications for water resources. *Water Resources Research,* 46(12): W12509.

Ohmura, A., 2001: Physical basis for the temperature-based melt-index method. *Journal of Applied Meteorology,* 40(4): 753-761.

Paterson, W. S. B., 1994: Physics of Glaciers. Tarrytown, NY: Pergamon Press, 480 pp.

Pederson, G. T., Graumlich, L. J., Fagre, D. B., Kipfer, T., and Muhlfeld, C. C., 2010: A century of climate and ecosystem change in western Montana: what do temperature trends portend? *Climatic Change,* 98(1): 133-154.

Pellicciotti, F., Brock, B., Strasser, U., Burlando, P., Funk, M., and Corripio, J., 2005: An enhanced temperature-index glacier melt model including the shortwave radiation

balance: development and testing for Haut Glacier d'Arolla, Switzerland. *Journal of Glaciology,* 51(175): 573-587.

Pellicciotti, F., Bauder, A., and Parola, M., 2010: Effect of glaciers on streamflow trends in the Swiss Alps. *Water Resources Research,* 46W10522.

Rieman, B. E., Isaak, D., Adams, S., Horan, D., Nagel, D., Luce, C., and Myers, D., 2007: Anticipated climate warming effects on bull trout habitats and populations across the interior Columbia River basin. *Transactions of the American Fisheries Society,* 136(6): 1552-1565.

Rothlisberger, H. and Lang, H., 1987: Glacial Hydrology. *In* Gurnell, A. M. and Clark, M. J. (eds.), Glacio-fluvial Sediment Transfer. New York, NY: Wiley, 207-284.

Selong, J. H., McMahon, T. E., Zale, A. V., and Barrows, F. T., 2001: Effect of temperature on growth and survival of bull trout, with application of an improved method for determining thermal tolerance in fishes. *Transactions of the American Fisheries Society,* 130(6): 1026-1037.

U.S. Bureau of Reclamation., 2012: St. Mary River-Milk River basin study draft report. Dept. of the Interior.

U.S. Fish and Wildlife Service., cited 2012: Endangered Species Profiles. [Available at: http://ecos.fws.gov/speciesProfile/profile/speciesProfile.action?spcode=E065#status].
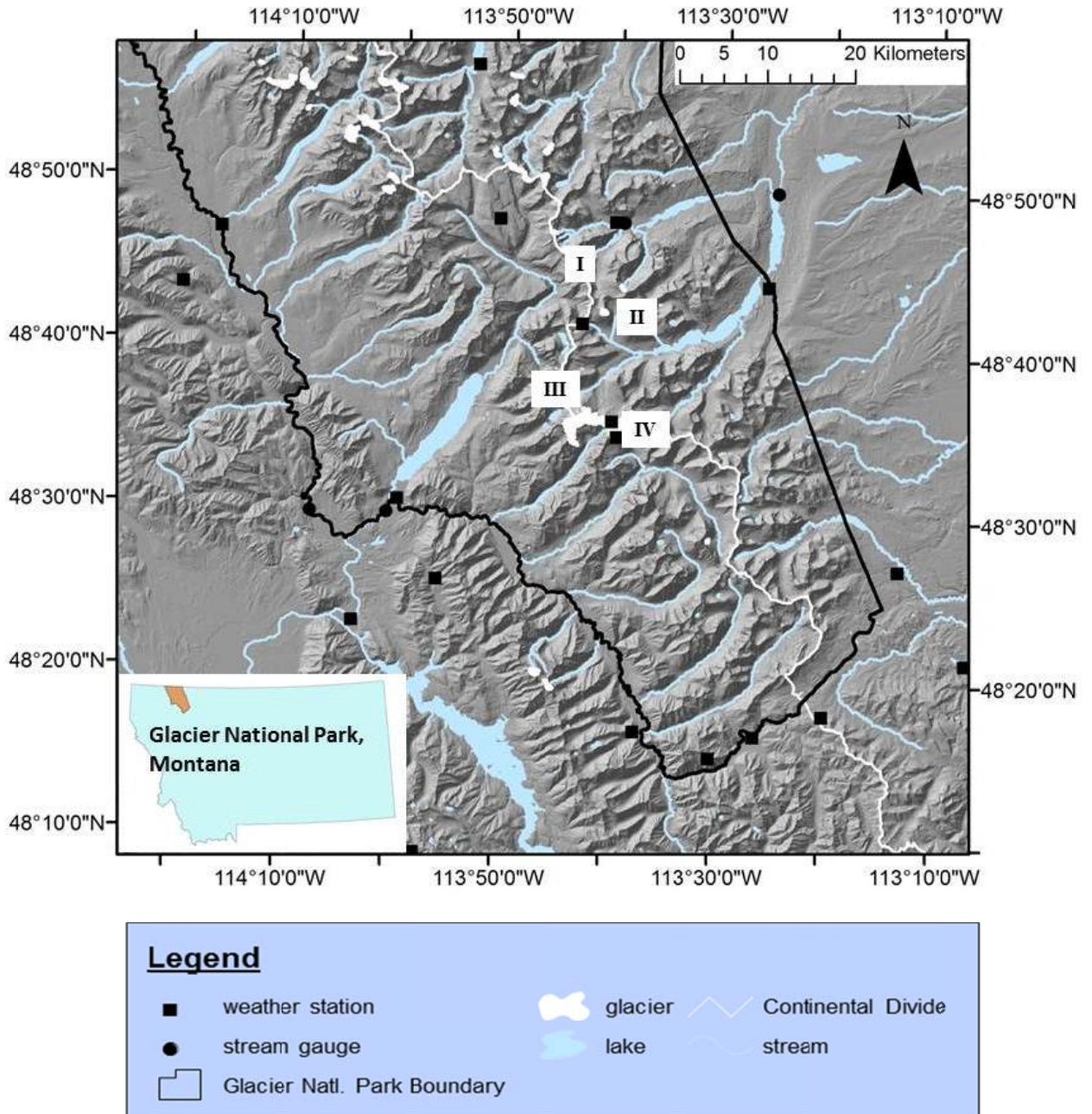
Figure 1 - Map of the study area showing the Glacier National Park boundary (black line), continental divide (white line), study glaciers (white, size exaggerated), weather stations (black squares, see Table 1), stream gauges (black circles, see Table 2), major streams and lakes (light blue). Roman numerals show approximate locations of the five study glaciers and correspond to the aerial photographs shown in Figure 3. Sperry Glacier, the site of the USGS mass balance monitoring program is located at numeral III.
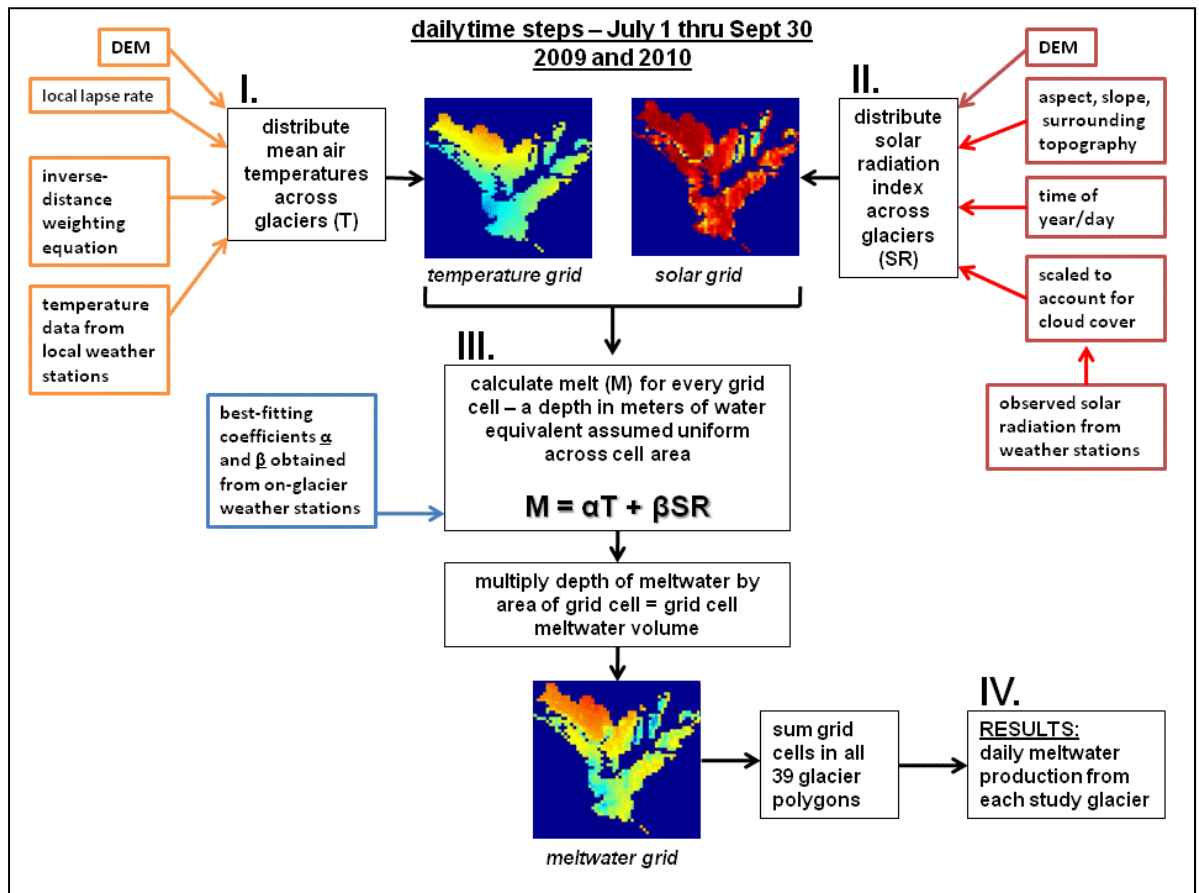
Figure 2 - Melt model flow chart illustrating the elements used to derive the temperature and solar radiation grids (parts I and II) used as model input. Melt is calculated in each grid cell and then multiplied by the grid cell area (3600 m^2) to yield a meltwater volume grid (part III). Lastly every grid cell within each glacier polygon is summed to give a daily meltwater volume for each of the 39 study glaciers. Here the grids corresponding to Blackfoot and Pumpelly Glaciers on August 1st, 2009 are given as examples.
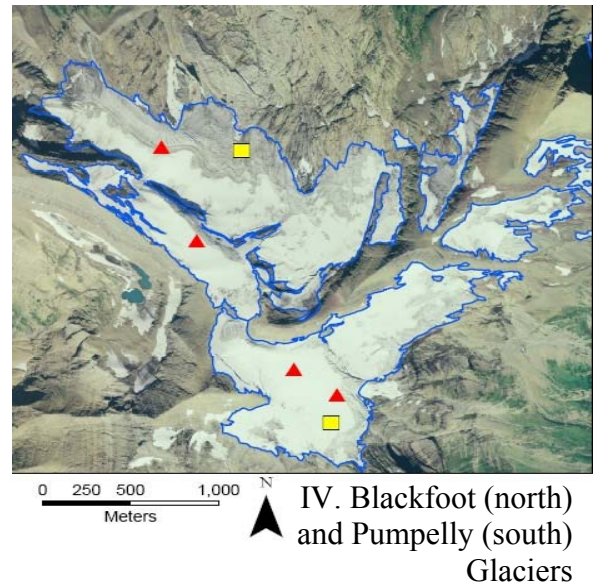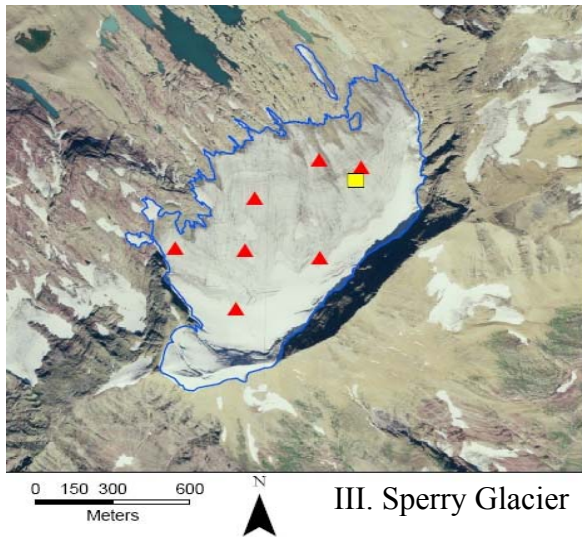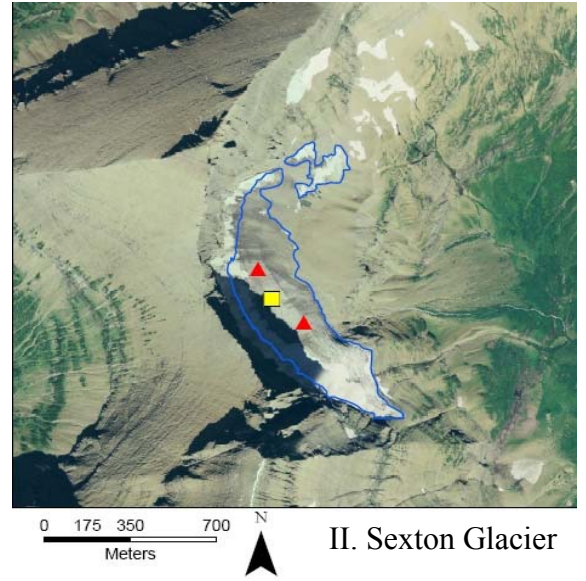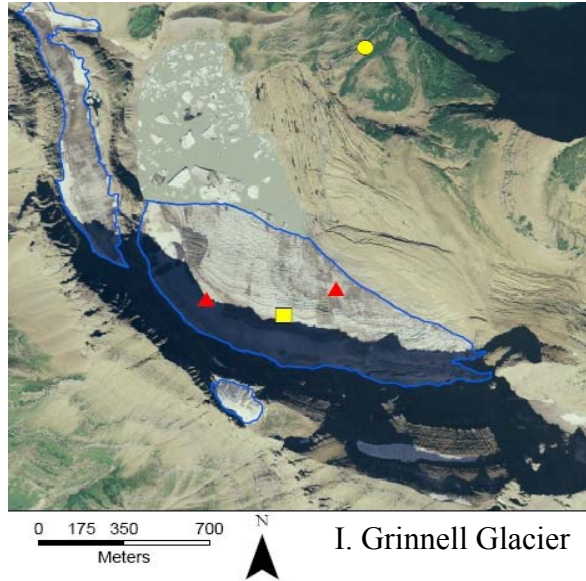
Figure 3 –Aerial photographs showing the five glaciers measured during summer
2010. Roman numerals correspond to the same in Figure 1 and show the locations
of these glaciers within the greater study area. Yellow squares show locations of
the on-ice weather stations and red triangles indicate an ablation stake. Blue lines
on the photos are the hand-digitized glacier margins
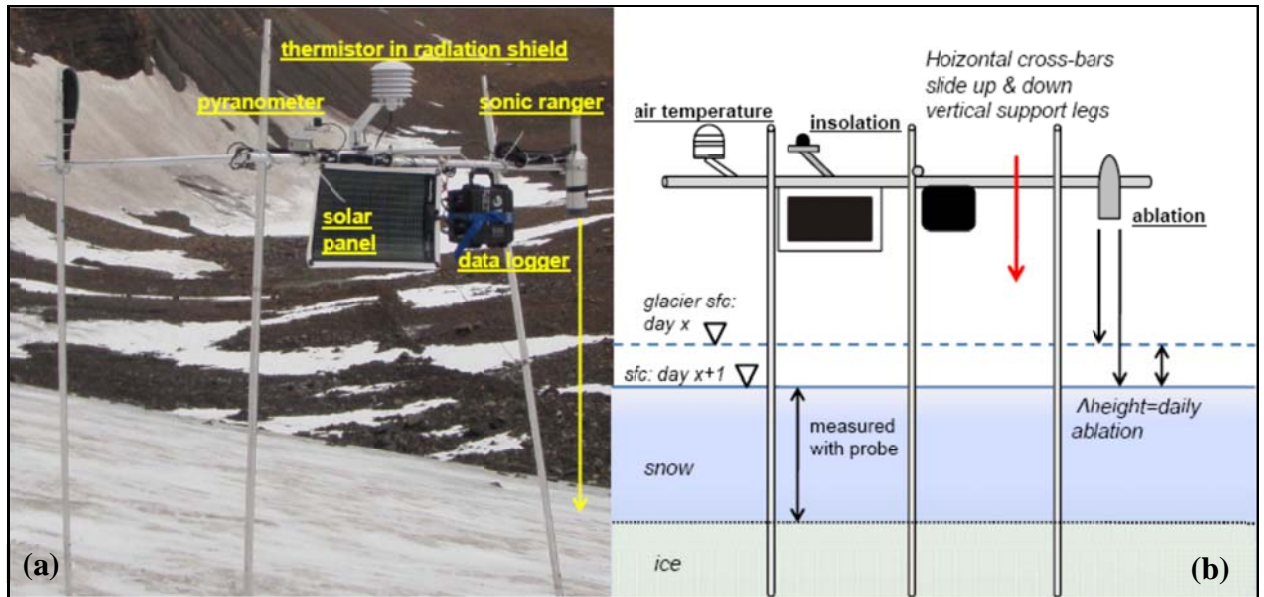
Figure 4 – Photograph (a) and schematic (b) (cross-section view) of an on-ice weather station showing the tower structure, and placement of the instruments, solar panel and data-logger. Stations had to be back-packable, so the tower structure was cut into 17, 150 cm long sections of 2.5 cm diameter aluminum pipe. We built each vertical leg by fastening five sections together in a telescoping fashion using roll pins and a 15 cm long aluminum rod at the joint. Two horizontal cross-bars forming a "T" connected the vertical legs above the glacier's surface. Instruments and a data-logger were fastened to these cross-bars. These cross-bars could be lowered down the vertical legs without un-fastening the instruments every 2-5 weeks in order to keep the increasingly top-heavy structure from falling over.
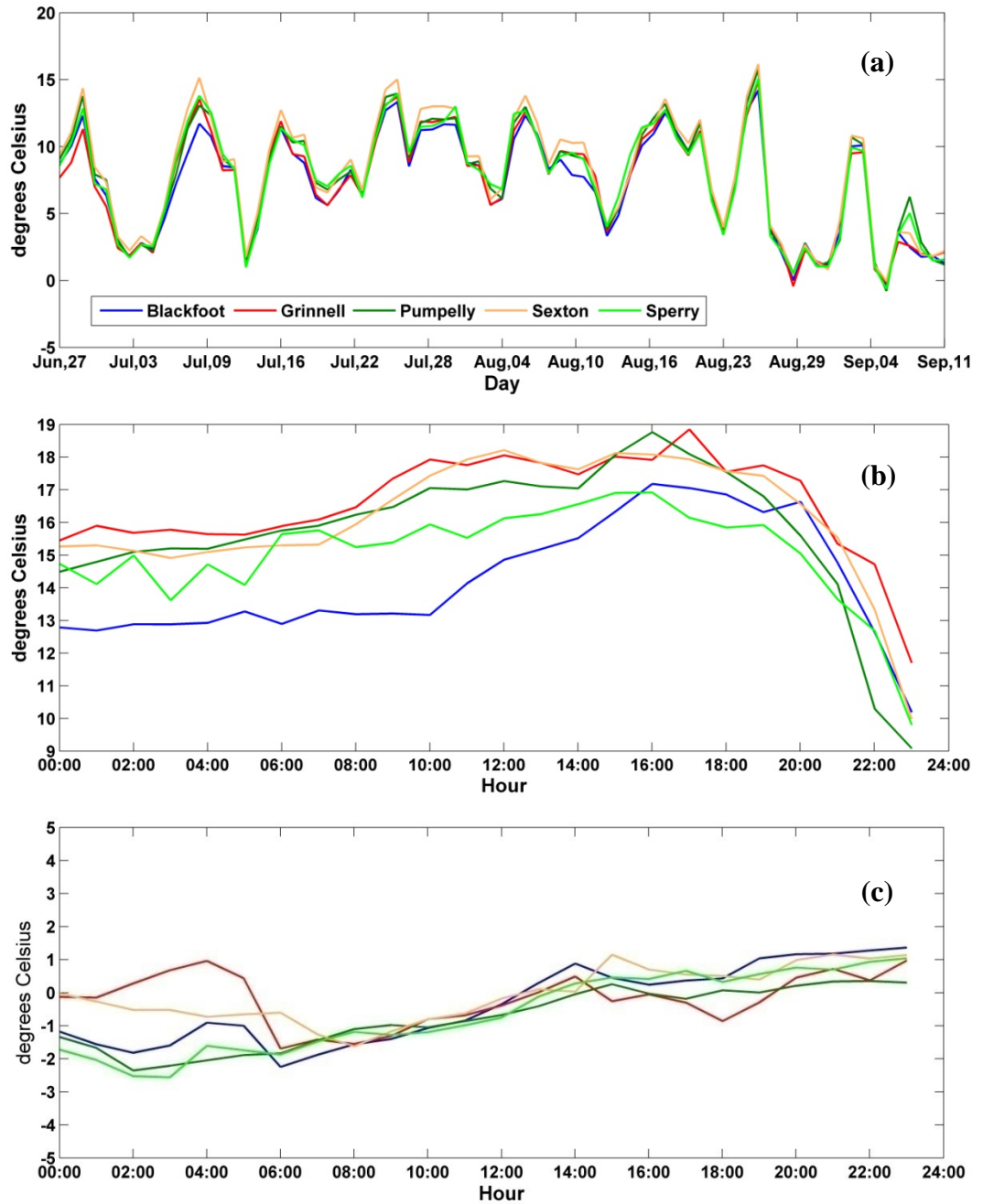
Figure 5 – (a) Time series plot of average daily temperatures during 2010 at the 5 on-glacier weather stations normalized by the mean elevation of these sites. (b) Normalized hourly temperatures from the 5 stations during the warmest day on record (8/26). (c) Normalized hourly temperatures during the coldest day on record (9/6)
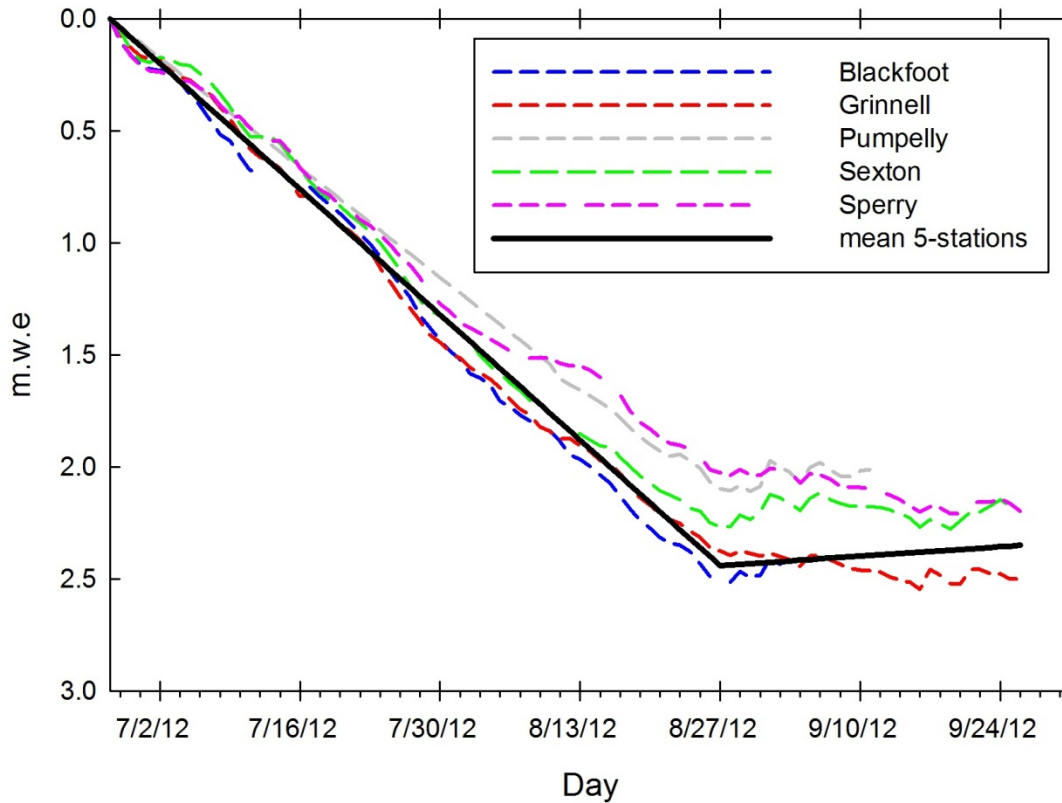
Figure 6 – Comparison of daily cumulative melt (surface lowering converted to water equivalent) measured with the sonic distance ranger at the five on-ice met stations, June 27th to September 26th, 2010 (dashed colored lines). The average melt rate between the five stations is plotted as a black solid line. A notable change occurs on 8/27. From 6/27-8/27 the average melt rate was 0.040 m d^{-1} w.e. but from 8/27-9/26, readings show the glaciers accumulated by an average rate of 0.003 m d^{-1} w.e. The sonic at the Pumpelly station only worked from 8/10 – 9/11, so we used an average rate of 0.040 m d^{-1} w.e. to generate the Pumpelly curve up to 8/10
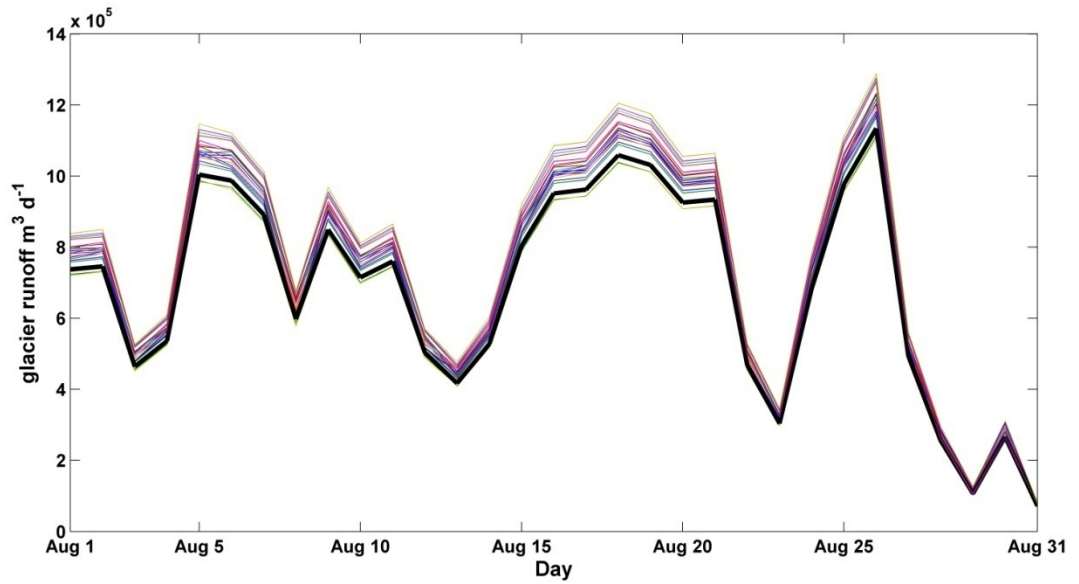
Figure 7 – Sensitivity to melt coefficient values. Time series plot of modeled August glacier runoff for the year 2010 using the chosen coefficients (thick black line) and the 20 other simulations as thin colored lines.

	North Fork	Middle Fork	Saint Mary	Swiftcurrent	Upper Grinnell
2009	6.3	7.5	12.7	27.7	109.1
2010	5.0	6.3	8.9	23.4	85.4
09-10 avg	5.6	6.9	10.7	25.6	98.2
1960s avg	6.8	7.9	12.7	30.9	85.0
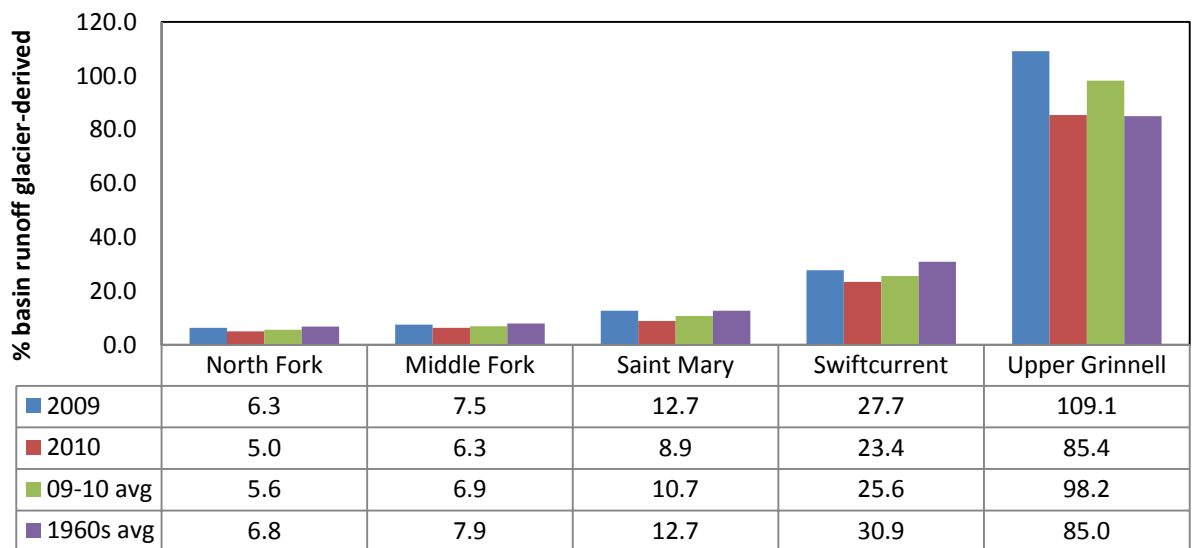
Figure 8 - The percentage of runoff that would be derived from glacier melt if all of it flowed through the stream gage. Values are given for the modeled years 2009 and 2010, the averaged value from these 2 years, and for the ten year period spanning 1960 - 1969.

38
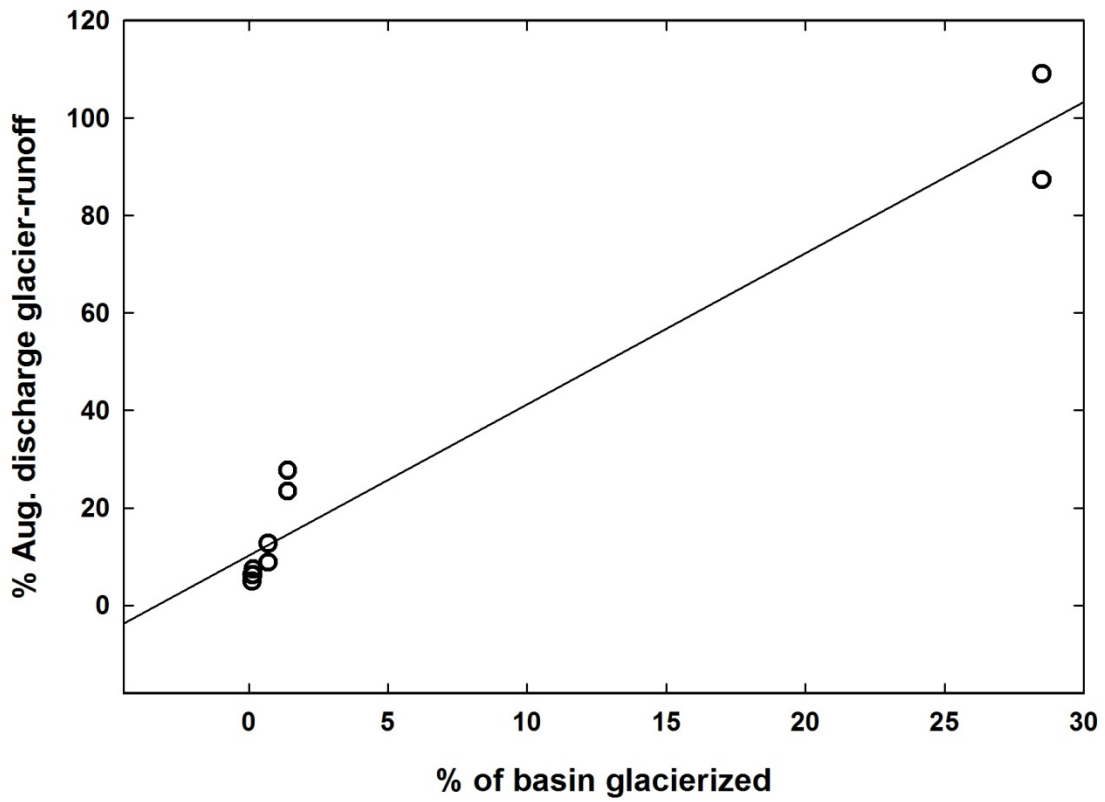
Figure 9 – The percentage the catchment area that is currently glacierized for each gauged basin plotted against the percentage of total basin runoff that could potentially come from glaciers during the months of August 2009 and 2010.
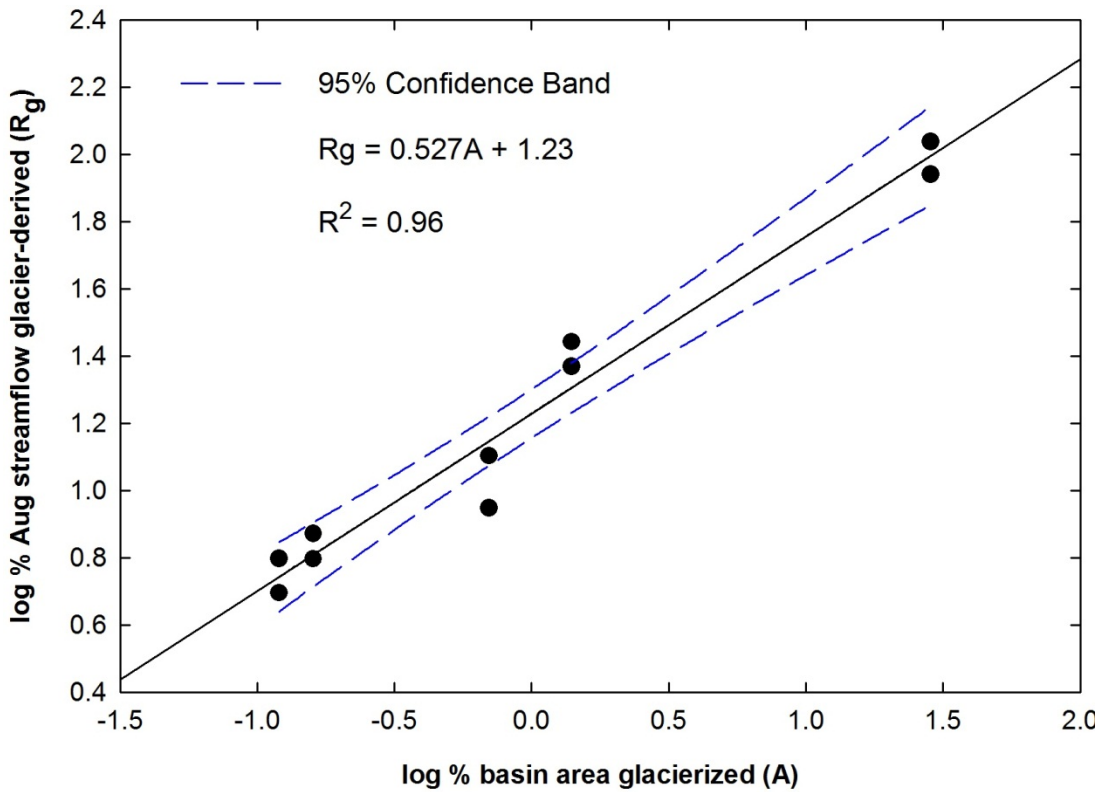
Figure 10 – Plot of the % glacierized area in the five study basins versus the % of total basin runoff that is potentially glacier-derived on log axes for Augusts 2009 and 2010. The relationship can be modeled well by the function $R_g = 0.527A+1.23$, where R_g is the log of the percentage of total basin runoff that could potentially come from glaciers and A is the log of the percentage of the basin glacierized. The estimated parameters were found to be statistically significant (p-values < 0.001) using a t-test and 95% confidence intervals.

Tables

Location Name	Source	Latitude	Longitude	Elevation (m)	Function(s)
Blackfoot Glacier*	Univ of MT Geosciences	48.5962	-113.6674	2214	lapse rate, temperature interpolation (2010), solar scaling (2010), deriving coefficients
Cyclone Ridge	MESOWEST	48.7242	-114.3358	1615	temperature interpolation (2009)
Deep Creek	RAWS	48.3556	-113.1139	1628	lapse rate, temperature interpolation (2009 & 2010), solar scaling (2009)
East Glacier	NCDC	48.4500	-113.2200	1465	lapse rate, temperature interpolation (2009 & 2010)
Emery Creek	SNOTEL	48.4300	-113.9300	1326	lapse rate, temperature interpolation (2009 & 2010)
Essex	NCDC	48.2800	-113.6200	1173	lapse rate, temperature interpolation (2009 & 2010)
Fielding	RAWS	48.2778	-113.4356	1402	temperature interpolation (2009 & 2010)
Flattop Mountain	SNOTEL	48.8000	-113.8500	1920	temperature interpolation (2009 & 2010)
Goat Haunt Mountain	MESOWEST	48.9567	-113.8903	1292	temperature interpolation (2009 & 2010)
Grinnell Glacier*	Univ of MT Geosciences	48.7502	-113.7263	2058	lapse rate, temperature interpolation (2010), solar scaling (2010), deriving coefficients
Hungry Horse Dam	NCDC	48.3847	-114.0575	983	lapse rate, temperature interpolation (2009 & 2010)
Kalispell Airport	NCDC	48.3000	-114.2700	906	temperature interpolation (2009 & 2010)
Logan Pass	MESOWEST	48.6949	-113.7169	2065	temperature interpolation (2009), solar scaling (2009)
Many Glacier	SNOTEL	48.8000	-113.6700	1494	temperature interpolation (2009 & 2010)
Noisy Basin	SNOTEL	48.1500	-113.9500	1841	temperature interpolation (2009 & 2010)
Pike Creek	SNOTEL	48.3000	-113.3300	1807	temperature interpolation (2009 & 2010)
Polebridge	RAWS	48.7825	-114.2803	1067	temperature interpolation (2009 & 2010), solar scaling (2009)
Pumpelly Glacier*	Univ of MT Geosciences	48.5800	-113.6591	2525	lapse rate, temperature interpolation (2010), solar scaling (2010), deriving coefficients
Saint Mary	NCDC	48.7375	-113.4306	1390	lapse rate, temperature interpolation (2009 & 2010), solar scaling (2009)
Sexton Glacier*	Univ of MT Geosciences	48.7005	-113.6352	2257	lapse rate, temperature interpolation (2010), solar scaling (2010), deriving coefficients
Snowslip	MESOWEST	48.2552	-113.5023	2140	temperature interpolation (2009)
Sperry Glacier*	Univ of MT Geosciences	48.6237	-113.7559	2383	lapse rate, temperature interpolation (2010), solar scaling (2010), deriving coefficients
West Glacier	NCDC	48.5106	-113.9942	975	lapse rate, temperature interpolation (2009 & 2010), solar scaling (2009)

* on-glacier weather station installed summer of 2010

Table 1 - Geographic data for weather stations with a description of how each was used in this study.

Basin	Period(s) of Record	Latitude	Longitude	Elevation (m)	catchment area (km^2)	present glacierized area km^2 (%-of basin)	mean August Q (m^3 s^{-1})	std dev August Q (m^3 s^{-1})	coefficient of variation (%)
North Fork Flathead River	1910-present	48.4926	-114.1257	959	3959.50	4.71 (0.12%)	45.32	14.32	32
Middle Fork Flathead River	1939-present	48.4955	-114.0102	954	2921.51	4.68 (0.16%)	37.82	12.01	32
Saint Mary River	1901-present	48.8426	-113.4230	1362	714.84	5.08 (0.7%)	27.18	6.02	22
Swiftcurrent Creek	1912-present	48.7997	-113.6568	1487	80.03	1.17 (1.4%)	3.26	0.96	29
Upper Grinnell Creek	1959-1971 & 2004-2007	48.7578	-113.7247	1920	2.85	0.81 (28.5%)	0.79	0.18	23

Table 2 – Geographic data for stream gauge sites, the associated watershed basins, and the mean and standard deviations for August discharge (Q) during the periods of record.

Location	Latitude	Longitude	Elevation (m)	Aspect (°)	Slope Angle (°)	6/27-7/27 mean daily melt/std dev (m.w.e.)	7/28-8/26 mean daily melt/std dev (m.w.e.)	8/27-9/26 mean daily melt/std dev (m.w.e.)	6/27-9/26 mean daily melt/std dev (m.w.e.)
[1]Blackfoot Glacier	48.5962	-113.6674	2214	50	11	0.048/0.014	0.044/0.017	no data	0.045/0.016
Grinnell Glacier	48.7502	-113.7263	2058	13	1	0.043/0.018	0.037/0.012	0.017/0.010	0.037/0.017
[2]Pumpelly Glacier	48.5800	-113.6591	2525	162	7	no data	0.033/0.010	no data	0.033/0.010
Sexton Glacier	48.7005	-113.6352	2257	54	28	0.037/0.017	0.034/0.016	0.016/0.012	0.030/0.018
Sperry Glacier	48.6237	-113.7559	2383	334	8	0.043/0.019	0.036/0.013	0.019/0.010	0.035/0.018
Combined Data		(mean)	2287			0.043/0.017	0.037/0.014	0.017/0.011	0.035/0.016

[1]Blackfoot Glacier station was operational only to Sep 11th. Much of Aug 27-Sep 11 melt data was thrown out due to the tower sinking into a small crevasse.

[2]Pumpelly Glacier sonic ranger was only operational from Aug 11th- early Sept.

Table 3 – Geographic data and mean daily melt rates reported with standard deviations (std dev) for the 5 on-glacier weather stations installed during 2010. Melt rates given as meters of of meltwater equivalent. The values under 8/27-9/26 use only observations from days when melt occured and do not include days when snowfall accumulated below the sonic ranger.

Stake	Latitude	Longitude	Aspect (°)	Slope Angle (°)	Elevation (m)	6/27-7/17 mean daily melt (m. w.e.)	7/10-8/16 mean daily melt (m.w.e.)	8/17-9/26 mean daily melt (m.w.e.)	6/27-9/26 mean daily melt (m.w.e.)	2010 cumulative melt (m.w.e.)
Blackfoot 1	48.5907	-113.6704	50	11	2,501	0.021	0.046	0.013	0.026	1.78
Blackfoot 2	48.5962	-113.6735	13	17	2,293	0.035	0.056	0.018	0.034	2.38
Grinnell 1	48.7507	-113.7307	15	13	2,057	0.036	0.042	no data	0.039	1.76
Grinnell 2	48.7514	-113.7235	341	13	2,041	0.044	0.052	0.025	0.040	3.29
Pumpelly 1	48.5831	-113.6623	136	15	2,622	0.029	0.044	0.014	0.027	1.88
Pumpelly 2	48.5817	-113.6588	123	8	2,552	0.027	0.047	0.014	0.027	1.89
Sexton 1	48.7017	-113.6361	54	26	2,256	no data	0.048	0.017	0.031	2.37
Sexton 2	48.6997	-113.6334	50	35	2,236	no data	0.042	0.017	0.028	2.15
Sperry 1	48.6247	-113.7583	357	17	2,391	0.044	0.044	0.018	0.034	2.74
Sperry 2	48.6264	-113.7551	349	13	2,345	0.043	0.042	0.016	0.033	2.62
Sperry 3	48.6225	-113.7587	20	14	2,468	0.044	0.033	no data	0.041	2.24
Sperry 4	48.6201	-113.7590	360	10	2,557	0.026	0.040	0.022	0.031	2.47
Sperry 5	48.6225	-113.7624	351	26	2,459	0.045	0.044	0.013	0.033	2.62
Sperry 6	48.6261	-113.7528	308	15	2,375	0.038	0.042	0.011	0.029	2.33
Sperry 7	48.6224	-113.7547	349	24	2,482	0.039	0.040	no data	0.039	1.96
Combine Stakes										
mean					2,376	0.036	0.044	0.017	0.033	2.30
standard deviation					174	0.008	0.005	0.004	0.005	0.42
median					2,391	0.038	0.044	0.017	0.033	2.33
min					2,041	0.021	0.033	0.011	0.026	1.76
max					2,622	0.045	0.056	0.025	0.041	3.29

Note time periods above overlap. The goal was to divide the ablation season into thirds, but the dates when stakes were checked slightly vary. Dates stakes were checked: Blackfoot & Pumpelly (7/3, 7/15, 8/9, 9/10), Grinnell (7/17, 8/12, 9/25), Sexton (7/10, 8/13, 9/26), Sperry (7/12, 8/16, 9/15).

Table 4 – Ablation stake data for the 15 stakes installed during 2010.

Run #	alpha	beta ($x10^{-6}$)	Δalpha	Δbeta	Δ August runoff	August Runoff (m^3 $x10^6$)
1	0.00365	3.62	-6%	-8%	-5%	20.76
2	0.00418	4.01	10%	2%	7%	23.52
3	0.00418	4.09	10%	4%	8%	23.67
4	0.00395	4.24	4%	8%	5%	23.08
5	0.00357	3.77	-4%	-4%	-5%	20.74
6	0.00372	4.24	-2%	8%	1%	22.19
7	0.00410	3.62	8%	-8%	3%	22.48
8	0.00418	4.17	10%	6%	9%	23.82
9	0.00380	4.32	0%	10%	3%	22.65
10	0.00403	3.85	6%	-2%	3%	22.64
11	0.00418	4.17	10%	6%	9%	23.82
12	0.00395	3.77	6%	-4%	1%	22.19
13	0.00410	3.85	8%	-2%	5%	22.91
14	0.00372	4.32	-2%	10%	2%	22.34
15	0.00380	3.85	0%	-2%	-1%	21.77
16	0.00403	4.01	6%	2%	5%	22.94
17	0.00372	3.69	-2%	-6%	-3%	21.16
18	0.00403	3.69	4%	-6%	2%	22.34
19	0.00418	4.32	10%	10%	10%	24.10
20	0.00418	3.54	10%	-10%	3%	22.64
chosen	0.00380	3.93	0%	0%	0%	21.92

Table 5 – List of the 20 different melt models showing the values for α and β, the changes from the chosen values of α and β, and the resultant change in total August runoff.

Basin	Period	% basin glacierized	Total glacier runoff ($m^3 mo^{-1}$, $x10^6$)	Total basin runoff ($m^3 mo^{-1}$, $x10^6$)	% basin runoff that could be glacier-derived
North Fork Flathead (NF)	2009	0.12	7.34	117.18	6.3
NF	2010	0.12	5.65	113.56	5.0
NF	mean 2009 & 2010	0.12	6.50	115.37	5.6
NF	mean 1960-1969	0.17	8.23	121.78	6.8
Middle Fork Flathead (MF)	2009	0.16	7.59	101.57	7.5
MF	2010	0.16	5.81	92.25	6.3
MF	mean 2009 & 2010	0.16	6.70	96.91	6.9
MF	mean 1960-1969	0.20	7.98	100.68	7.9
Saint Mary (SM)	2009	0.7	9.04	71.06	12.7
SM	2010	0.7	7.00	78.89	8.9
SM	mean 2009 & 2010	0.7	8.02	74.975	10.7
SM	mean 1960-1969	1	10.43	81.84	12.7
[1]Swiftcurrent (SW)	2009	1.4	2.12	7.66	27.7
SW	2010	1.4	1.70	7.28	23.4
SW	mean 2009 & 2010	1.4	1.91	7.47	25.6
SW	mean 1960-1969	2.1	2.53	8.18	30.9
[2]Upper Grinnell Creek (GC)	2009	28.5	1.57	1.44	109.1
GC	2010	28.5	1.23	1.44	85.4
GC	mean 2009 & 2010	28.5	1.42	1.44	98.6
GC	mean 1960-1969	44.7	1.93	2.27	85.0

[1]Swiftcurrent is a sub-basin of the Saint Mary basin

[2]Upper Grinnell Creek is a sub-basin of the Swiftcurrent basin

Table 6 – Percent of glacier-derived runoff within the 5 gauged watersheds for the month of August.

APPENDIX: SUPPLEMENTARY INFORMATION

A. Model Input: Temperature Index

To obtain a mean daily air temperature for each grid cell we created an interpolated temperature surface for the model domain using an inverse-distance weighting equation.

$$T_{gc} = [\Sigma_i(v_i/d_i^2)] \, / \, [\Sigma_i(1.0/d_i^2)] \qquad \text{(A1)}$$

Where:

T_{gc} = daily mean temperature for the grid cell, $°C$

v_i = measured daily mean temperature for the ith nearest neighbor, $°C$

d_i = distance to the ith nearest neighbor, m

A local linear lapse rate of -0.0074 $°C$ m^{-1} was calculated using data from the on-glacier weather stations and six low elevation (<1500 m) weather stations that are either inside the Park or within 12 km of the border (Table 1). The temperatures at each weather station are first converted to their respective sea level equivalents using the local lapse rate and the DEM. Equation A1 generates the temperature surface across the model domain. This surface is then adjusted back to the proper temperatures for the corresponding altitude using the same lapse rate and the elevations given by the model DEM.

In an effort to investigate the error associated with this process, the data from the five on-glacier weather stations were removed and then the interpolation was ran again for the summer of 2010. The new interpolated temperatures for the grid cells containing

the on-glacier weather stations were then compared to the measured values.

B. Model Input: Solar Radiation Index

To obtain a solar radiation index for each glacierized grid cell we first calculated the potential direct solar radiation that each cell would receive under perfectly clear-sky conditions (Equation A2) [*Hock*, 1999].

$$SR_p = [I_o(R_m/R)^2 a^{\left(\frac{P}{P_o \cos Z}\right)} \cos\theta] \qquad (A2)$$

Where I_o is the solar constant (1368 Wm^2), a is the mean atmospheric emissivity under clear sky conditions, we assumed a value of 0.75 (Hock, 1999). P is the atmospheric pressure over the grid cell which is obtained from the DEM and the local lapse rate. P_o is the mean atmospheric pressure at sea level (101,300 Pa). $(R_m/R)^2$ is the Earth's orbital eccentricity correction factor which is time dependent. R is the instantaneous Sun-Earth distance and R_m is the mean Sun-Earth distance. Here $(R_m/R)^2$ is approximated by Equation.

$$(R_m/R)^2 = 1.00011 + 0.034221cos(\gamma) + 0.00128sin(\gamma) + 0.000719cos(2\gamma) +$$
$$0.000077sin(2\gamma) \quad (A3)$$

Where $\gamma = 2\pi n/365$ radians and $n =$ Julian day of the year.

Z is the local zenith angle and θ is the angle of incidence between the normal to the grid slope and the solar beam. $Cos\theta$ is determined using Equation .

$$cos\theta = cos(b)cos(Z) + sin(b)sin(Z)cos(azsum - azslope) \quad \text{(A4)}$$

Where *b* is the grid cell slope angle, *azsun* is the solar azimuth, and *azslope* is the slope

azimuth (equal to the grid cell slope). Shading from the surrounding terrain is accounted

for and radiation equals zero between sunset and sunrise. Equations A3 and A4 calculate

an average radiation value on hourly time steps which are then summed for each day to

supply a potential solar radiation index SR_p (W m^{-2}).

While using the above methods takes into account the variables that control

radiation input as a result of geographic location and time; the amount of radiation

actually received on the ground is often much less than the potential. Hence, there would

be less energy available for melt (Figure A1). This is often due to local weather systems

and the cloud cover that blocks the incoming solar radiation from the top of the

atmosphere.
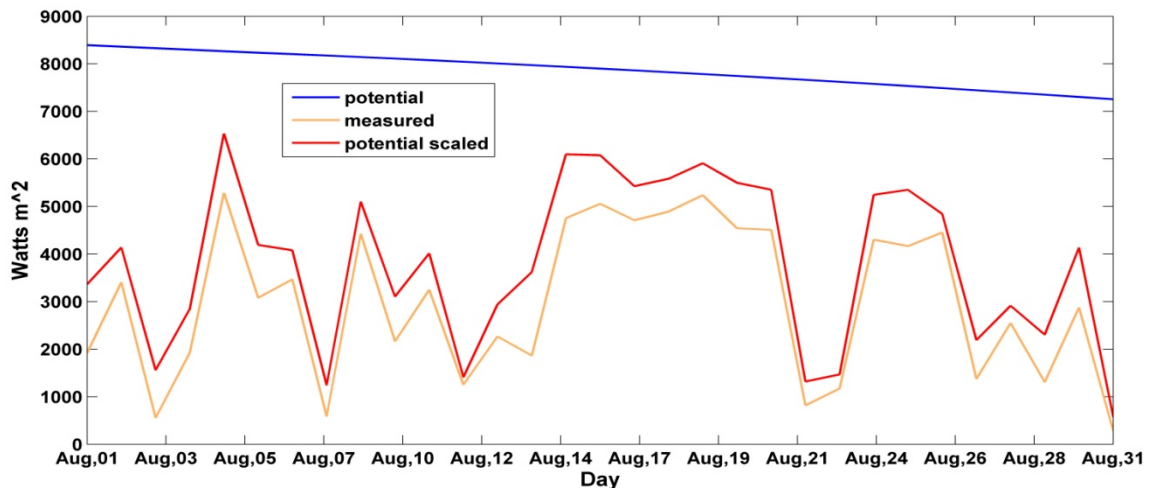
Figure A1 – Time series plot of the potential solar radiation, the measured solar radiation, and the potential radiation after it was scaled for the month (the model input) at Grinnell Glacier during August, 2010.

We found model performance improved when we dealt with this discrepancy by multiplying SR_p by a daily scaling factor. This factor was obtained using local weather station data taken at five different sites with insolation observations (Table 1). We first compared the daily measured solar radiation against the potential radiation computed for that weather station's respective grid cell. The measured value divided by the potential revealed what percentage of the potential radiation actually reached the ground. Observations from the five on-ice weather stations indicate relatively little variation across the landscape in the amount of radiation received for each day (Figure A2).
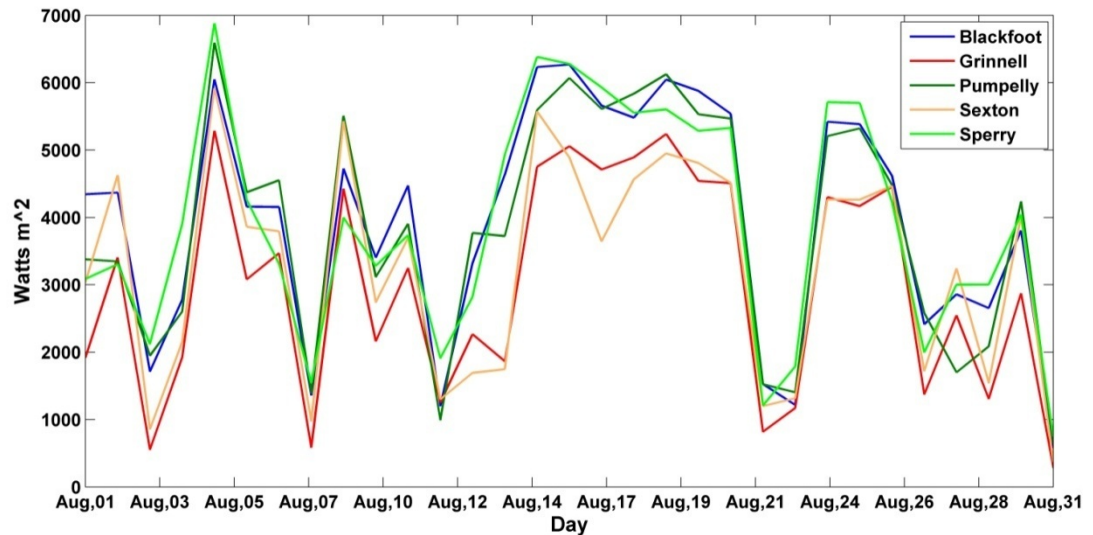
Figure A2 – Time series plot of measured solar radiation on the five study glaciers during 2010.

Thus, we derived the scaling factor by taking the average of the percentages obtained at the weather stations for every day. For example on August 15th, 2010 the station on Blackfoot Glacier recieved 77% of the potential radiation, Grinnell 60%, Pumpelly 73%, Sexton 79%, and Sperry 95%. So the scaling factor for this day was 0.77. Next, every potential radiation value in each grid cell was multiplied by 0.77. This created the radiation index for August 15th, 2010.

C. Table A1 - List of Study Glaciers

Glacier Name	Latitude	Longitude	1966 Area km^2	2005 Area km^2	1966-2005 % change in area	2005 Mean Elevation (m)
Agassiz Glacier	48.9339	-114.1595	1.59	1.04	-35	2,464
Ahern Glacier	48.8426	-113.7839	0.59	0.51	-13	2,503
Baby Glacier	48.9054	-114.1542	0.12	0.08	-34	2,059
Blackfoot Glacier	48.5938	-113.6669	2.33	1.79	-23	2,388
Boulder Glacier	48.9570	-114.0894	0.23	0.06	-76	2,418
Carter Glacier	48.8894	-114.0501	0.27	0.20	-26	2,388
Chaney Glacier	48.8520	-113.8305	0.54	0.38	-29	2,296
Dixon Glacier	48.9299	-114.0158	0.45	0.28	-38	2,360
Gem Glacier	48.7467	-113.7286	0.03	0.02	-18	2,488
Grant Glacier	48.3241	-113.7514	0.35	0.29	-18	2,420
Grinnell Glacier	48.7509	-113.7261	1.02	0.62	-40	2,088
Harris Glacier	48.9497	-114.2313	0.15	0.04	-74	1,978
Harrison Glacier	48.5889	-113.7290	2.07	1.89	-9	2,494
Herbst Glacier	48.9857	-114.0513	0.17	0.06	-63	2,227
Hudson Glacier	48.9639	-114.0453	0.10	0.03	-66	2,223
Ipasha Glacier	48.8424	-113.8131	0.32	0.21	-34	2,339
Jackson Glacier	48.5990	-113.7023	1.54	1.18	-23	2,408
Kintla Glacier	48.9297	-114.1939	1.73	1.14	-34	2,540
Logan Glacier	48.6014	-113.6332	0.50	0.30	-40	2,232
Lupfer Glacier	48.4773	-113.5130	0.14	0.07	-51	1,941
Miche Wabun Glacier	48.9459	-113.8307	0.30	0.13	-56	2,212
N. Swiftcurrent Glacier	48.7879	-113.7661	0.12	0.08	-32	2,148
Old Sun Glacier	48.8715	-113.7799	0.42	0.37	-12	2,730
Piegan Glacier	48.7075	-113.6845	0.28	0.25	-10	2,533
Pumpelly Glacier	48.5860	-113.6555	1.49	1.26	-16	2,485
Rainbow Glacier	48.8807	-114.0861	1.28	1.16	-9	2,532
Red Eagle Glacier	48.5915	-113.6181	0.21	0.11	-48	2,189
Salamander Glacier	48.7571	-113.7384	0.23	0.17	-23	2,192
Sexton Glacier	48.7007	-113.6338	0.40	0.28	-31	2,250
Shepard Glacier	48.8657	-113.8592	0.25	0.11	-56	2,284
Siyeh Glacier	48.7329	-113.6573	0.22	0.06	-74	2,181
Sperry Glacier	48.6235	-113.7566	1.34	0.87	-35	2,460
Stanton Glacier	48.3377	-113.7736	0.53	0.31	-42	2,475
Swiftcurrent Glacier	48.7688	-113.7459	0.26	0.22	-14	2,232
Thunderbird Glacier	48.9345	-114.0377	0.36	0.24	-33	2,353
Two Ocean Glacier	48.8376	-114.0189	0.43	0.28	-36	2,576
Vulture Glacier	48.8252	-114.0261	0.65	0.37	-43	2,558
Weasel Collar Glacier	48.8948	-114.0657	0.59	0.55	-7	2,328
Whitecrow Glacier	48.9207	-113.8362	0.37	0.20	-47	2,170
All 39 Glaciers						
Total			23.97	17.20	-28	
Mean			0.61	0.44	-35	2,337
Standard Deviation			0.59	0.48	19	176
Median			0.37	0.28	-34	2,353
Minimum			0.03	0.02	-76	1,941
Maximum			2.33	1.89	-7	2,730

D. Description of Gauged Watersheds

Of the basins with current stream gauge data, the North Fork (NF) of the Flathead River is the largest at 3,960 km^2. It also has the lowest percentage of glacierized area at 0.12% for the present day. The Middle Fork (MF) of the Flathead basin is the second largest with a total catchment area of 2,922 km^2 with currently 0.16% of this covered by ice. These two basins combined drain all the glacier-derived runoff occurring west of the continental divide. The Saint Mary River (SM) watershed is the third largest basin (715 km^2) and sits east of the continental divide with 0.7% of catchment glacierized today. Streamflow here travels down to the South Saskatchewan River and eventually out to Hudson Bay. The Swiftcurrent Creek (SW) basin (80 km^2) is actually a sub-basin of the Saint Mary but was singled out because it has the highest amount of glacierized area (currently at 1.4%) of the four basins with stream gauge records for 2009 and 2010. The Upper Grinnell Creek site (GC) measures runoff from a catchment that is 2.9 km^2 with 28.5% of this area currently covered by glacier. It has two periods of record spanning the years 2004-2007 and 1959-1971. This is the only high-elevation, first order basin inside the study area with a stream gauge record, making it highly desirable for our analysis. This catchment is a sub-basin of the Swiftcurrent Creek watershed, and the gauge sits within 500 meters of Grinnell Glacier, the largest of three glaciers in the basin. Here a small (0.33 km^2) pro-glacial lake sits between the stream gauge and the terminus of this glacier. For the period of record spanning 2004-2007, we used the average August discharge to represent the total basin runoff for 2009 and 2010.

E. Table A2 - Local weather observations on the min/max melt day

| Weather Station	Mean Aug temperature (°C)	2009				2010			
		Aug 15 (minimum melt)		Aug 22 (maximum melt)		Aug 31 (minimum melt)		Aug 26 (maximum melt)	
		avg temp (°C)	precip (mm)	avg temp (°C)	precip (mm)	avg temp (°C)	precip (mm)	avg temp (°C)	precip (mm)
Emery Ck	13.5	8.6	7.6	18.5	0.0	7.8	2.5	15.2	0.0
Flattop	11.5	5.7	12.7	17.1	0.0	4.6	0.0	13.5	0.0
Pike Ck	14.0	7.8	0.0	17.6	0.0	7.2	2.5	18.7	0.0
Many Glacier	14.5	8.7	5.1	19.6	0.0	8.4	2.5	17.4	2.5
West Glacier	16.5	10.0	5.1	19.4	0.0	8.9	3.7	16.7	0.0
Polebridge	14.5	9.6	0.0	15.8	0.0	7.4	0.8	18.0	0.0
Saint Mary	14.5	10.0	2.8	19.4	0.0	8.8	0.3	15.6	1.5
Fielding	15.0	7.5	3.8	19.3	0.0	5.6	5.6	19.1	0.0
Sperry Margin	8.0	1.7	ND	15.2	ND	-0.6	ND	14.8	ND
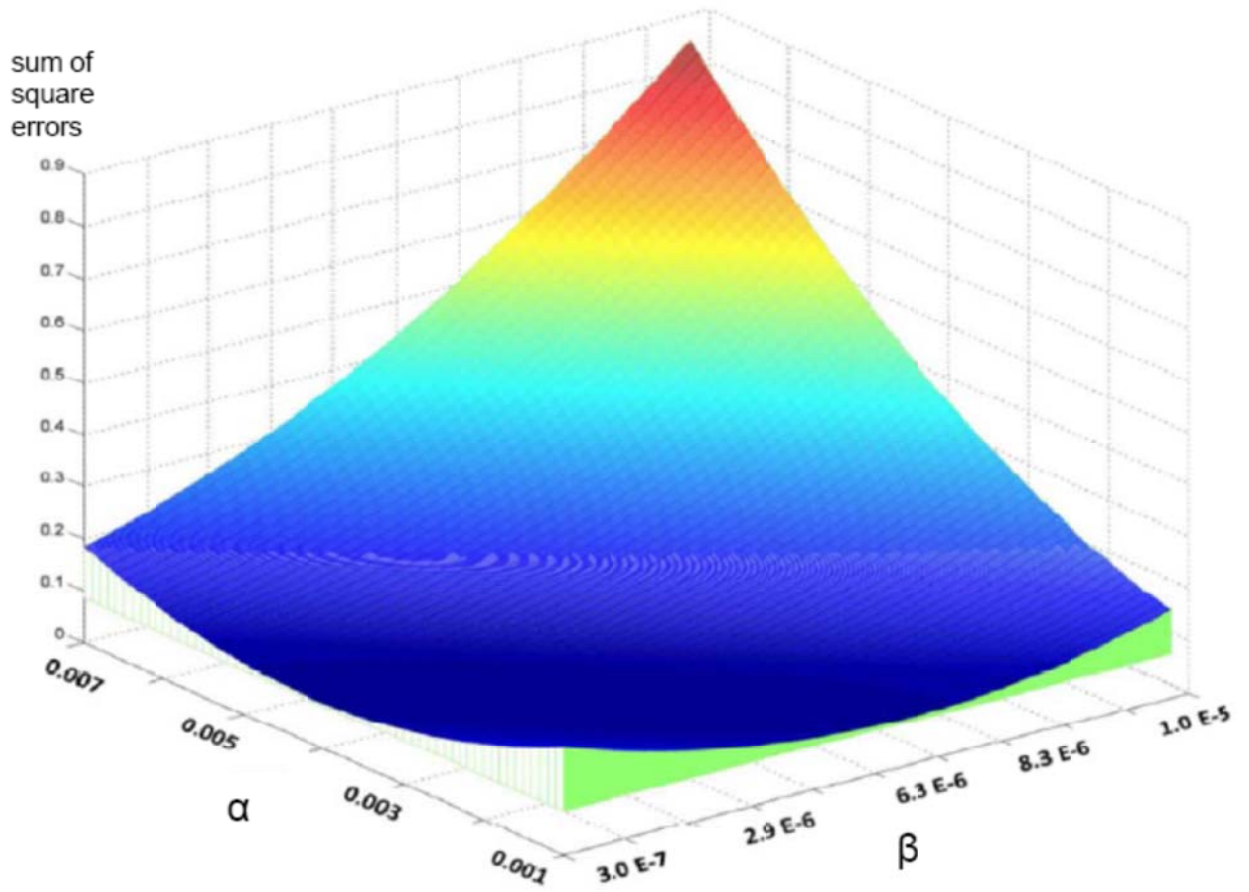
Figure A3 - Plot of the error-space generated from equation 2 and then used to obtain the melt model coefficients.

G. Table A3 - List of August runoff and specific discharges for the 39 study glaciers

Glacier Name	2005 Area km^2	2009		2010	
		August total (m^3 x 10^6)	August specific discharge (m)	August total (m^3 x 10^6)	August specific discharge (m)
Agassiz Glacier	1.04	1.65	1.59	1.27	1.23
Ahern Glacier	0.51	0.83	1.62	0.65	1.27
Baby Glacier	0.08	0.15	1.93	0.12	1.55
Blackfoot Glacier	1.79	3.04	1.70	2.30	1.29
Boulder Glacier	0.06	0.07	1.35	0.06	1.04
Carter Glacier	0.20	0.34	1.69	0.27	1.31
Chaney Glacier	0.38	0.64	1.68	0.51	1.35
Dixon Glacier	0.28	0.43	1.53	0.33	1.19
Gem Glacier	0.02	0.04	1.50	0.03	1.13
Grant Glacier	0.29	0.48	1.68	0.42	1.48
Grinnell Glacier	0.62	1.23	2.00	0.99	1.60
Harris Glacier	0.04	0.08	1.91	0.06	1.55
Harrison Glacier	1.89	3.03	1.61	2.27	1.20
Herbst Glacier	0.06	0.10	1.61	0.08	1.27
Hudson Glacier	0.03	0.04	1.26	0.03	1.00
Ipasha Glacier	0.21	0.38	1.79	0.30	1.44
Jackson Glacier	1.18	2.11	1.79	1.61	1.36
Kintla Glacier	1.14	1.61	1.42	1.23	1.08
Logan Glacier	0.30	0.55	1.83	0.43	1.42
Lupfer Glacier	0.07	0.15	2.16	0.12	1.84
Miche Wabun Glacier	0.13	0.23	1.72	0.18	1.36
N. Swiftcurrent Glacier	0.08	0.15	1.92	0.12	1.57
Old Sun Glacier	0.37	0.51	1.39	0.39	1.05
Piegan Glacier	0.25	0.41	1.64	0.31	1.24
Pumpelly Glacier	1.26	2.02	1.61	1.50	1.20
Rainbow Glacier	1.16	1.83	1.57	1.39	1.20
Red Eagle Glacier	0.11	0.21	1.96	0.17	1.54
Salamander Glacier	0.17	0.31	1.78	0.24	1.42
Sexton Glacier	0.28	0.49	1.77	0.40	1.44
Shepard Glacier	0.11	0.19	1.73	0.15	1.37
Siyeh Glacier	0.06	0.10	1.78	0.08	1.43
Sperry Glacier	0.87	1.43	1.63	1.07	1.22
Stanton Glacier	0.31	0.48	1.58	0.42	1.36
Swiftcurrent Glacier	0.22	0.40	1.79	0.32	1.44
Thunderbird Glacier	0.24	0.37	1.57	0.29	1.23
Two Ocean Glacier	0.28	0.43	1.55	0.33	1.18
Vulture Glacier	0.37	0.55	1.49	0.42	1.14
Weasel Collar Glacier	0.55	0.97	1.76	0.77	1.40
Whitecrow Glacier	0.20	0.34	1.75	0.27	1.39
Combine Glaciers	17.20	28.37	1.68 (mean)	21.92	1.33 (mean)

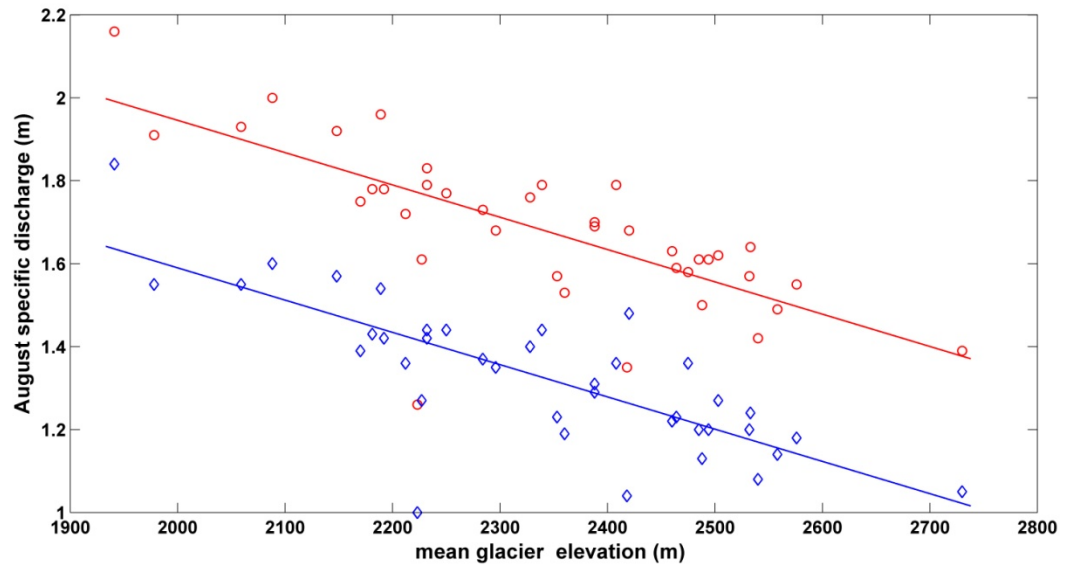## H. Correlation Between Glacier Elevation and August melt

Figure A4 - Plot of mean glacier elevation versus monthly specific discharge for both August 2009 (red circles) and 2010 (blue diamonds). Each point represents a glacier's mean elevation (x-axis) and its average specific discharge, which can be thought of as a monthly melt rate (y-axis). Correlations exist, but are not particularly strong with R^2 values of 0.55 in 2009 and 0.60 in 2010. P-values for both data sets were <0.001

I. North Fork Flathead Water Temperature Calorimetry Equation

The effect of glacier-melt on water temperatures in the North Fork River at the stream gauge can be examined by setting up a calorimetry equation.

$$T_t = \frac{m_g c_w T_g + m_{ng} c_w T_{ng}}{m_t c_w} \qquad (A5)$$

Where T_t is "total" temperature of the combined glacier and non-glacier runoff, in this case the measured North Fork value of 15 °C. T_g and T_{ng} are the temperatures of the

glacier (assumed 0°C) and the non-glacier components. c_w is the specific heat of water

(4186 J/kg°C), m_t is the mass of the combined glacier and non-glacier streams (based off

mean August discharge, this equals 1.23 x 10^{11} kg), m_g is the mass of glacier component

(6.16 x 10^9 kg, assuming 5% of total runoff), m_{ng} is the mass of non-glacier component

(1.17 x 10^{11} kg). Factoring out c_w and re-arranging to solve for T_{ng}, the only unknown

variable in the equation yields equation A6.

$$T_{ng} = \frac{m_t T_t - m_g T_g}{m_{ng}} \tag{A6}$$

The result is a value of 15.8 °C for T_{ng}, an increase in temperature of 5%, meaning that, if

the glacier runoff were removed from the North Fork River, then T_t would increase to

15.8 °C at the stream gauge.